Secondary User Interference Characterization for Spatially Random Underlay Networks with Massive MIMO and Power Control

S. Kusaladharma and C. Tellambura, *Fellow*, *IEEE*

***Abstract*—In an underlay (secondary) network, the receiver nodes are subject to both primary and intra underlay interference. What are the characteristics of this interference when considering the use of massive MIMO (Multiple Input Multiple Output) systems with pilot contamination, path-loss-inversion power control, receiver association policies, spatially random nodes and propagation characteristics with power-law path loss and Rayleigh fading? To answer this question, we derive the average and the moment generating function (MGF) of the aggregate interference and its average due to both primary and underlay transmissions from nodes modeled as Poisson point processes and analyze how the interference impacts the outage performance of an underlay receiver. Our analysis considers all of the above factors and both single antenna type and massive MIMO base stations. We show that massive MIMO improves the outage performance, and a higher path loss exponent reduces the outage probability. This is in contrast to single antenna systems where a higher path loss exponent increases the outage. Furthermore, it is shown that the different node densities and power thresholds significantly affect the outage performance.**

I. Introduction

The aggregate interference on the receiver of a cognitive (unlicensed) user (CU) is one of the most fundamental performance limiting factors. The interference will reduce the achievable data rate and reliability (e.g., increasing outage). However, it is the direct result of allowing simultaneous spectrum access for both primary users (PUs) and CUs. But this is the fundamental premise of the underlay paradigm [3], a candidate for future fifth generation (5G) wireless systems, device-to-device (D2D) communications, sensor networks, and cognitive femtocells in heterogeneous networks [4]–[6]. Since cognitive radio (CR) underlay networks operate on an interference tolerant basis [4], [7], mitigating the interference on PU nodes via exclusion regions around PU receivers [8], maximum underlay transmit power thresholds, and interference temperature based channel access is the primary research focus of many works. In contrast, the aggregate interference on a CU receiver from PU and other CU transmissions has not been analyzed in detail.

This aggregate interference on a CU receiver constitutes two main parts (i) PU-to-CU interference and (ii) CU-to-CU interference. Both these interference terms depend on how transmitting nodes control their power, their receiver association policies, and their random locations. The interference depends on both large-scale and small-scale fading as well. Can this interference on a CU receiver be controlled by using spatial degrees of freedom? To this end, massive multiple input multiple output (MIMO) systems, with extremely large antenna arrays, provide exciting prospects [9]. For instance, the integration of CR and massive MIMO cancels interference via the use of excessive spatial degrees of freedom, provides simultaneous service to a large number of users, increases spectral and energy efficiencies, and negates the effects of small scale fading and noise [4]. However, the successful integration faces technical challenges. The fundamental challenge of massive MIMO is the need for extensive channel state information (CSI) for the different transmitter-receiver links. In a time domain duplexing (TDD) set-up, channel reciprocity is exploited, and the CSI is commonly obtained via periodic uplink pilot transmissions. However, the length of the pilots are practically constrained by the channel coherence time[1] and the acceptable pilot overhead[2]. Therefore, the number of orthogonal pilots are limited, and pilot reuse by different base stations in both primary and CU networks leads to pilot contamination which generates focused interference to the links using the same pilot sequence. Pilot contamination is a fundamental bottleneck in massive MIMO systems, which limits the potential spectral and throughput gains [9]. Overall, all these factors and in turn the aggregate interference tightly depends on spatial randomness of the nodes, which must be modeled via stochastic geometry tools. Thus, statistical characterization of the aggregate interference on a CU receiver using stochastic geometry approaches is the focus of this paper.

A. Problem statement and Contribution

In this paper, we derive the statistics of the aggregate interference on a CU receiver node due to both PU and CU transmissions, and investigate its impact on the performance. We will incorporate pilot contamination (when base stations employ massive MIMO), spatial randomness of nodes, power control and receiver association procedures, and channel imperfections.

Our study is motivated by a number of questions. While interference issues in underlay CR networks have been extensively investigated, for analytical tractability, it is not uncom-

The authors are with the Department of Electrical and Computer Engineering, University of Alberta, Edmonton, AB, Canada T6G 2V4. (Email: kusaladh@ualberta.ca and chintha@ece.ualberta.ca)

This paper was presented in part at the IEEE International Communications Conference (ICC), Kuala Lumpur, Malaysia, 2016 [1] and at the IEEE Vehicular Technology Conference (VTC-Fall), Boston, MA, USA, 2015 [2].

[1]This is the time period in which the channel response can be assumed to be constant. For standards like LTE and UMTS, this is practically in the range of 1-2 ms [10].

[2]The proportion of symbols within the coherence time used for pilot transmissions is an overhead because it does not lead to any effective data transfer.

mon to ignore power control and receiver association schemes, and omitting spatial randomness [11]–[15]. How do these assumptions affect of the overall interference levels? Moreover, how do we characterize the aggregate interference when there are massive MIMO enabled base stations with power control techniques? Furthermore, how do we incorporate a network of PU and CU nodes where the locations and numbers of transmitter/receiver nodes are random without restricting the system model to a single PU transmitter receiver pair or a single cell with one massive MIMO enabled base station?

To further investigate such questions, in this paper, we begin by representing PU nodes (transmitters and receivers) with two independent homogeneous Poisson point processes in $\mathbb{R}^2$ (Fig. 1). We will consider two models for the underlay system: 1) a Matern cluster process with the underlay base stations representing the cluster heads distributed as a homogeneous Poisson point process, and 2) underlay base stations and receivers distributed in $\mathbb{R}^2$ as independent homogeneous Poisson point process. However, the PU receiver nodes have exclusion zones around them. When a CU transmitter falls within this zone, it has to stay silent.

The base stations are either single antenna or equipped with massive MIMO, with CSI being obtained via uplink pilots. Log distance path loss and independent Rayleigh fading are assumed for all channels. Furthermore path loss inversion based power control is considered. While channel inversion or feedback based power control schemes exist [16], they are beyond the scope of this paper. PU receivers associate with their closest base station. For the underlay system, we consider three association schemes: 1) a transmitter initiates a connection with the closest receiver, 2) a receiver initiates an association with the closest transmitter, and 3) the receiver associates with the base station at the cluster head. We characterize the performance of an associated CU receiver by deriving the moment generating function (MGF) of the aggregate interference for the single antenna case, and the MGF, mean, and variance of the normalized aggregate interference for the massive MIMO case along with the outage probability.

B. Prior research

Extensive interference characterization and modelling of underlay networks includes developing analytical results based on the MGF, moments, cumulants, outage, and coverage. For instance, [17] develops interference models considering power control, contention control, and hybrid power-contention control schemes. The success probability, spatial average rate, and area spectral efficiency are derived for cellular and underlay D2D users under Rician fading [18], and it is shown that these measures depend on user density, channel propagation parameters, and spectrum occupancy ratios. The authors in [18] further propose a centralized opportunistic access control scheme as well as a mode selection mechanism to reduce cross tier interference. An analytical framework to characterize the area spectral efficiency of a large Poisson underlay CU network is proposed in [19]. The authors highlight shaping medium access and transmit power as available degrees of freedom in designing the CU network, and shows that an area spectral efficiency wall exists. Furthermore, [20] proposes an adaptive power control scheme for CU systems in a Rayleigh fading channel which maximizes the output signal to noise ratio (SNR) and the interference, and shows that this scheme can achieve up to a 3 dB SNR gain. Reference [21] proposes a limited feedback based underlay spectrum sharing scheme for Poisson cognitive networks, with the benefit that the secondary area spectral efficiency increases with the secondary outage constraint. Moreover, interference on a PU receiver is characterized [22] by considering constraints on a secondary (underlay) transmitter from both primary and secondary systems.

Name	PDF
$Lin(\alpha)$	$f(x) = \frac{2x}{\alpha^2},\ 0 < x < \alpha$
$Ral(\alpha)$	$f(x) = 2\alpha x e^{-\alpha x^2},\ 0 < x < \infty$
$TRal(\alpha, \beta)$	$f(x) = \frac{2\alpha x e^{-\alpha x^2}}{1-e^{-\alpha\beta^2}},\ 0 < x < \beta$

TABLE I: List of commonly used PDFs.

The integration of massive MIMO and underlay CR is an emerging research area. Thus, interference issues in randomly deployed massive MIMO base stations are investigated in [11], [23]–[27]. For example, the interference from massive MIMO enabled cellular networks to D2D networks is studied in [26] under perfect and imperfect CSI at the receivers. With perfect CSI, it is observed that underlay contamination arises in addition to pilot contamination. The trade-offs between the average sum rate and energy efficiency is studied in [27], and in order for these parameters to improve from the high number of antennas, the number of cellular users should be a function of the number of base station antennas. Moreover, in order for massive MIMO and underlay D2D to coexist, the density of D2D users must be low. Reference [25] derives closed-form expressions for the base station density bounded by the maximum outage probability and concludes that the base station density must be below a certain bound to fulfill coverage requirements, while [11] obtains signal-to-interference-ratio expressions for both uplink and downlink under orthogonal and non-orthogonal pilot sequences and shows that the downlink signal to interference ratio is limited by the inverse of the total pilot correlation. Furthermore, the uplink of a wireless network using linear minimum mean square error spatial processing is analyzed in [23], and the distribution of the spectral efficiency in the interference limited regime is derived. Moreover, [24] analyzes the coverage probability and area spectral efficiency for a heterogeneous network showing that significant throughput gains can be achieved by interference nulling and co-ordination among the tiers.

Notations: $\Gamma(x, a) = \int_a^\infty t^{x-1}e^{-t}dt$ and $\Gamma(x) = \Gamma(x, 0)$ [28]. $\Pr[A]$ is the probability of event A, $f_X(\cdot)$ is the probability density function (PDF), $F_X(\cdot)$ is the cumulative distribution function (CDF), $M_X(\cdot)$ is the MGF, and $\mathbb{E}_X[\cdot]$ denotes the expectation over random variable X. Furthermore, notations for commonly used PDFs are summarized in Table I while notations for frequently used symbols are depicted in Table II.

Name	PDF
$\Phi_{p,t}$	PPP of PU transmitters
$\lambda_{p,t}$	PU transmitter density
$\Phi_{p,r}$	PPP of PU receivers
$\lambda_{p,r}$	PU receiver density
R_G	Guard region radius
$\Phi_{u,t}$	PPP of CU transmitters
$\lambda_{u,t}$	CU transmitter density
$\Phi_{u,r}$	PPP of CU receivers
$\lambda_{u,r}$	CU receiver density
d_l	Cluster diameter
$g(r)$	Channel power gain due to path loss at distance r
α	Path loss exponent
κ	Ratio between PU and CU transmitter antennas
$P_*, * \in \{u, p, \{p,u\}, \{p,p\}\}$	Receiver sensitivity of CU receivers, PU receivers, and CU and PU pilots
$\lambda_{u,t}$	Density of active CU transmitters
$\lambda_{p,t}$	Density of active PU transmitters
η	Probability of a PU transmitter using the a-th pilot
θ	Probability of a CU transmitter using the a-th pilot
$\tilde{\theta}$	Probability of a CU transmitter not being within a guard region
q	Number of orthogonal pilots
D	Maximum allowable transmission distance
σ^2	Noise variance
T	Threshold SINR required for detection
I_p	Interference from PUs
I_u	Interference from CUs

TABLE II: List of commonly used symbols.

II. System model and Assumptions

A. Spatial Model

This section describes the spatial distribution of primary and underlay nodes.

1) Primary Network: A single class of PU transmitters (base stations) distributed randomly in $\mathbb{R}^2$ is considered. Although node locations in actuality are not purely random (e.g. base station locations are planned), a point process can accurately approximate even planned node placements while providing analytical tractability [29], [30]. The Poisson point process model has thus been extensively used to model base station locations [17], [31]–[33] for cognitive, D2D, and heterogeneous networks. Thus, to develop a general analysis and to avoid special cases, we assume homogeneous Poisson point processes for both PU transmitters and receivers.

Let the PU transmitters be distributed as a stationary homogeneous Poisson point process $\Phi_{p,t}$ with intensity $\lambda_{p,t} > 0$. Due to the homogeneity of $\Phi_{p,t}$, $\lambda_{p,t}$ is a constant over all $\mathbb{R}^2$. The number of PU transmitters within any closed area $\mathcal{B}$ follows the Poisson distribution with [34]

$$\Pr[N(\mathcal{B}) = n] = \frac{(\lambda_{p,t}\mathcal{B})^n}{n!} e^{-\lambda_{p,t}\mathcal{B}}. \quad (1)$$

The PU receivers are also modeled similarly and denoted by $\Phi_{p,r}$ with spatial intensity $\lambda_{p,r} > 0$. $\Phi_{p,r}$ and $\Phi_{p,t}$ are considered to be independent, stationary, and motion invariant. Moreover, the PU receiver locations are independent of PU transmitters.

One significant aspect of underlay networks is the guard (exclusion) region [15], [33]. This physical region around either the PU transmitters or the PU receivers precludes CU transmissions. It therefore helps to ensure that the PU interference is controlled. CUs may learn its existence through a centralized process where dynamic location information is made available through the network itself, or via a distributed mechanism where each CU senses the spectrum for pilot signals transmitted from the PU receivers [15]. Both these processes lead to CUs maintaining a silence within guard regions. Therefore, we will assume that a guard region exists around each PU receiver having a constant radius of R_G, and that the CUs perfectly know it.

2) Underlay Network: For this, we will consider two separate configurations. For both configurations, it is assumed that the CU devices are spatially independent from the primary transmitters and receivers.

- *Cluster model*:
  In this configuration, we will model this network as a Matern cluster process [35]–[37]. This model consists of multiple node clusters centered around underlay base stations [36]. The Matern Cluster process is formally defined as follows [37]. Let $\Phi_{u,t} = \{a_1, a_2, a_3...\}$ be a homogeneous Poisson point process representing cluster centers with intensity $\lambda_{u,t} > 0$, and B_i is a set of Poisson point processes conditional on $\Phi_{u,t}$ centred on a_i $(\forall i)$ where each B_i is independent of each other and stationary. The resulting cluster process $\Phi_{u,r} = \cup_i B_i$ is a Matern cluster process if B_i is uniformly distributed within a ball $b(a_i, d_l)$ with density $\lambda_{u,r}$ centred at a_i and having a radius $\frac{d_l}{2}$. The cluster centers correspond to base stations while the daughter processes correspond to the receivers. The cluster radii, admission of receivers, and scheduling within the clusters are dependent on the specific network parameters. A wireless local area network or a nano/pico cell base station are examples where clustering could occur [37] for the CU network.
- *Voronoi model*:
  Here, the CU base stations and receivers are distributed randomly in $\mathbb{R}^2$ as two independent and stationary homogeneous Poisson point processes $\Phi_{u,t}$ and $\Phi_{u,r}$ with spatial densities $\lambda_{u,t}$ and $\lambda_{u,r}$. Although the assumption of transmitter-only and receiver-only devices holds true for primary networks, underlay networks can have devices which may switch from being a transmitter to a receiver and vice versa. The voronoi model is useful for analyzing wireless ad-hoc networks and dual macro-micro cell networks. Moreover, this model is also useful whenever a set of wireless local area and pico cell base stations belonging to the same network cover a particular area.

B. Signal model

Universal frequency reuse is assumed within the primary network. All channel power gains are independent and identically distributed and are independent of the underlying point

processes. While the path loss is power-law, small scale fading is modelled as Rayleigh. The channel power gain $|h|^2$ is thus distributed as $f_{|h|^2}(x) = e^{-x}, 0 < x < \infty$. From the simplified path loss model [38], the received power P_R at a distance r from the transmitter is $P_R = Pg(r)$ with $g(r) = r^{-\alpha}$, where P is the transmit power level and α is the path loss exponent. Practically, α can range from around $2-6$, and the special case of $\alpha = 2$ occurs when the propagation is through free space [39]. However, α values slightly less than 2 may occur in tunnels due to the wave guide effect. But, having $g(r) = r^{-\alpha}$ creates analytical complications when $r < 1$. Thus, for tractability, we will also use $g(r) = \min(1, r^{-\alpha})$ [40] where necessary. Since spatial densities are small, the probability of having a device within 1m is negligible, and both forms of $g(r)$ will yield the same results.

1) Multiple antenna case: Both CU and PU receivers are single antenna devices while PU transmitters and CU transmitters have M and N antennas respectively, which are constant. M and N have the relationship $M = \kappa N$. M and N are assumed to be large enough to serve all associated users. A time division duplex (TDD) scheme is assumed for both primary and underlay networks [11].

Both primary and CU networks utilize pilots in the uplink channel to estimate CSI for the downlink. The pilots are of length L, and are mutually orthogonal. That is, pilot sequences satisfy $x_a^* x_b = 0$ whenever $a \neq b$, where $x_a, x_b \in \mathbb{C}^{L\times 1}$ are pilot sequences. We assume a set of q orthogonal pilots, which is used by all base stations; both primary and underlay [11]. We assume that the training phase for all base stations occur simultaneously regardless of whether they are part of the primary or underlay network [11]. These assumptions lead to the maximum level of pilot contamination. Furthermore, the channel gains are static between the training phase and the downlink data transmission phase.

C. Power control and transmitter-receiver association

Both primary and CU transmitters employ path loss inversion based power control to ensure a fixed average power[3] at their receivers [17]. Note however that the instantaneous received power fluctuates due to small scale fading. Thus, the transmit power P_T becomes $P_T = P_* r^\alpha$, where r is the transmitter-receiver distance, α is the path loss exponent, and $* \in \{u, p, \{p, u\}, \{p, p\}\}$ denote underlay, primary, underlay pilots, and primary pilots. This form of power control ensures that all receivers reach the same received power, where receivers close to the transmitters are not at an unfair advantage. Moreover, for the multiple antenna case, power scaling is employed by the primary and underlay base stations where the downlink transmitted signal is scaled by $\frac{1}{\sqrt{M}}$ and $\frac{1}{\sqrt{N}}$ respectively to compensate for the number of transmitter antennas. While normalizing the precoding vector can also be implemented [41], [42], to provide more realistic results, we defer this for future work.

In the primary network, the PU receiver associates with the closest PU transmitter (base station). Such association provides the best average received power. With this scheme, the PU transmitters form Voronoi cells[4] (shown in Fig. 1), and associate with intra-cell receivers. However, within a time-frequency block, there can only be one receiver associated with the transmitter. Other receivers who initiate transmission would be assigned separate resource blocks if available. We assume that there is always a receiver connected to the transmitter within the resource block in question because the PU transmitter density $\lambda_{p,t}$ is considered to be significantly lower than the PU receiver density $\lambda_{p,r}$. This assumption provides the maximum level of interference.

For the underlay network, we consider several association schemes. These are categorized according to the number of antennas at a CU transmitter:

- *Single antenna case*
  Here, we consider 2 different association policies for the Voronoi model: 1) the receiver initiates communication and selects the closest available transmitter, and 2) the transmitter initiates the communication and selects the closest available receiver. These policies are valid for networks such as ad-hoc and D2D networks (Case 1 corresponds with a typical cellular mobile or digital TV user while case 2 corresponds with an ad-hoc or sensor network). We assume that all available transmitters (with a density of $\bar{\lambda}_{u,t}$) are associated with receivers, and occurrences of multiple transmitters associating with a single receiver are permissible. For both aforementioned schemes, the selection of transmitters and receivers only occurs whenever they are within a distance of D from the initiating receiver or transmitter. The maximum allowable distance D ensures that the transmit power level would not increase beyond the maximum possible power level, and is analogous to having a maximum cut-off power level.
  For the cluster model, the receivers associate with their cluster head (parent node).
- *Multiple antenna case*
  Underlay association schemes for the multiple antenna case are as follows. With a cluster model, the associated base station is the cluster head, while with a Voronoi model, the receivers associate with the closest base station similar to the association policy of the primary network. In a scenario where the transmitter has a large number of antennas, it is a fully fledged base station, and not part of an ad-hoc network. Therefore, situations where transmitters initiate the communication procedure in the downlink are rare, and transmitters would have sufficient power which makes the maximum allowable distance irrelevant.

III. Outage analysis for the single antenna case

Within this section, we derive the outage probability of an active CU receiver along with the MGF of the interference. We assume that the receiver is associated with a transmitter successfully.

[3]This power level can either be the receiver sensitivity or the receiver sensitivity plus an appropriate fade margin.

[4]A voronoi tessellation divides an area of $\mathbb{R}^2$ into different regions depending on the distance to a specific set of nodes. For each node, its corresponding voronoi cell consists of points which are closer to it than to any other node

Let r be the distance between the CU receiver and the associated transmitter. The received power P_R may be written as $P_R = P_u r^{\alpha} r^{-\alpha} |h|^2 = P_u |h|^2$. Thus, given that an association has occurred, neither the association policy for the underlay network nor r play any role in the received power. However, other CU and all PU transmissions generate interference. Let I_p, I_u, and σ^2 be the interference from the primary and underlay networks, and the noise variance respectively. The signal to interference and noise ratio (SINR) at the CU receiver (γ) is written as $\gamma = \frac{P_u |h|^2}{I_p + I_u + \sigma^2}$. The CDF of the SINR ($F_\gamma(x)$) can be written as

$$F_\gamma(x) = 1 - e^{(-\frac{x\sigma^2}{P_u})} M_{I_p}\left(\frac{x}{P_u}\right) M_{I_u}\left(\frac{x}{P_u}\right). \quad (2)$$

Substituting the required SINR threshold (T) instead of x gives us the outage probability. However, in order to evaluate this, the MGFs of I_p and I_u are needed, which will be derived next. The MGF can also be used to calculate additional statistics of the interference such as thoughput and bit error rate [43]–[45].

A. Interference from the primary network

The primary interference on the CU receiver can be written as $I_p = \sum_{i \in \Phi_{p,t}} I_{p,i}$, where $I_{p,i}$ is the interference from the i-th PU transmitter. We can write $I_{p,i}$ as $I_{p,i} = P_P |h|^2 r_p^{-\alpha}$, where P_P is the transmit power of a PU transmitter and r_p is its distance to the CU receiver in question. Without the loss of generality, we consider this CU receiver to be at the origin. A useful trick is mapping the intensity function from 2-D to 1-D to provide better mathematical tractability. Therefore, using the Mapping Theorem [46], the 1-D intensity of the PU transmitters with respect to the CU receiver ($\tilde{\lambda}_{p,t}$) can be written as $\tilde{\lambda}_{p,t} = 2\pi\lambda_{p,t} r_p$.

The MGF of I_p is defined as $M_{I_p}(s) = \mathbb{E}[e^{-sI_p}]$. By the Campbell's theorem [46], $M_{I_p}(s)$ is written as

$$M_{I_p}(s) = e^{\left(\int_0^\infty \mathbb{E}\left[e^{-sP_P|h|^2 r_p^{-\alpha}} - 1\right] 2\pi\lambda_{p,t} r_p dr_p\right)}, \quad (3)$$

where the expectation is with respect to $|h|^2$ and P_P. The evaluation of (3) requires the distribution of P_P. However, due to the distance dependent power control, $P_P = P_p r_{p,tx}^{\alpha}$, where the distance between a PU transmitter, and the associated receiver is $r_{p,tx}$. Thus, the problem is to find the distribution of $r_{p,tx}$.

However, finding the exact distribution of $r_{p,tx}$ is difficult, and thus we will approximate it. We assume that $r_{p,tx}$ is independent from the distances to other PU transmitters. However, as the PU network forms voronoi cells and because each voronoi cell has only a single PU transmitter as its nucleus, coupling is introduced between the cells [47]. As such $r_{p,tx}$ is correlated with corresponding transmitter-receiver distances within other voronoi cells. Furthermore, the probability that there are no receivers associated with a given transmitter is greater than zero. However, this probability is negligible when the primary receiver density is much larger than the primary transmitter density ($\lambda_{p,r} >> \lambda_{p,t}$), which is the case in practice.

Thus, using the distribution of the nearest node from a point within a PPP [48], the distance $r_{p,tx}$ is approximately distributed with the PDF $f_{r_{p,tx}}(x) = 2\pi\lambda_{p,t} x e^{-\pi\lambda_{p,t} x^2}$ which is given by $Ral(\pi\lambda_{p,t})$ (see Appendix I for proof). To verify the accuracy of this PDF, Fig. 2 compares the theoretical CDF of $r_{p,tx}$ with simulated CDFs for two different PU transmitter densities ($\lambda_{p,t}$). It is seen that the discrepancy under $\lambda_{p,t} = 1\times10^{-5}$ is lower than that when $\lambda_{p,t} = 1\times10^{-6}$. Moreover, it should be noted that more accurate results may be obtained by introducing a scaling factor to the Rayleigh distribution as was done in [47], [49].

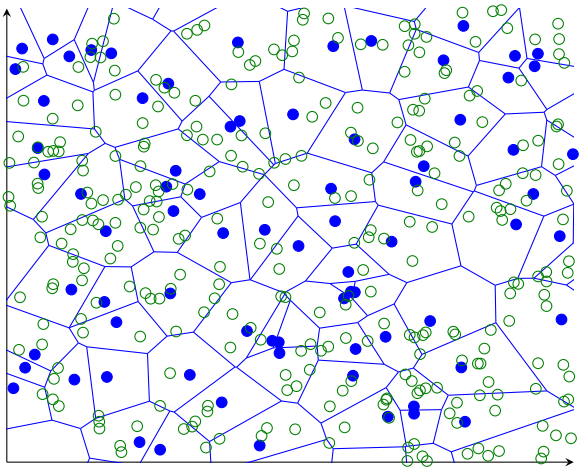

Fig. 1: Primary network layout: blue circles = PU transmitters, and green circles = PU receivers. The PU transmitters and receivers are distributed as independent homogeneous Poisson point processes. The receivers within each voronoi cell connect to the corresponding transmitter. Note that underlay nodes are not shown.

Coming back to the original objective of finding $M_{I_p}(s)$, we can perform the expectation on (3) with respect to $|h|^2$ and obtain $M_{I_p}(s) = e^{\left(\int_0^\infty \mathbb{E}\left[\frac{1}{1+sP_p r_{p,tx}^{\alpha} r_p^{-\alpha}} - 1\right] 2\pi\lambda_{p,t} r_p dr_p\right)}$, where the remaining expectation is with respect to $r_{p,tx}$. When $\alpha > 2$, changing the order of integration and averaging results in

$$M_{I_p}(s) = e^{\left(-\frac{2\pi^2\lambda_{p,t}}{\alpha} \frac{(sP_p)^{\frac{2}{\alpha}}}{\sin\left(\frac{2\pi}{\alpha}\right)} \mathbb{E}\left[r_{p,tx}^2\right]\right)} = e^{\left(-\frac{2\pi}{\alpha} \frac{(sP_p)^{\frac{2}{\alpha}}}{\sin\left(\frac{2\pi}{\alpha}\right)}\right)}. \quad (4)$$

The mean interference $\mathbb{E}[I_p]$ is another important performance measure. $\mathbb{E}[I_p]$ can be used to gauge the severity of interference affecting a particular device. Furthermore, $\mathbb{E}[I_p]$ is also vital when approximating the interference to another well-known distribution, or when simplifying the interference component when calculating an approximation for the outage. From the Campbell's theorem [46], we can write

$$\mathbb{E}[I_p] = \int_0^\infty \mathbb{E}_{|h|^2, r_{p,tx}}\left[P_p |h|^2 r_{p,tx}^{\alpha} r_p^{-\alpha}\right] 2\pi\lambda_{p,t} r_p dr_p. \quad (5)$$

The integration in (5) does not necessarily converge because the simplified path loss model does not hold when $r_p < 1$, and thus we take $g(r) = \min(1, r^{-\alpha})$ as illustrated in Section II B. Moreover, in practical channels $\alpha > 2$. Using these facts and breaking the integration in (5) into two separate parts, we obtain $\mathbb{E}[I_p]$ in closed-form as

$$\mathbb{E}[I_p] = 2P_p \frac{\Gamma(\frac{\alpha}{2}+1)}{(\pi\lambda_{p,t})^{\frac{\alpha}{2}-1}} \left(\frac{1}{\alpha-2} + \frac{1}{2}\right). \quad (6)$$

It should be noted that 6 does not hold when $\alpha \leq 2$.

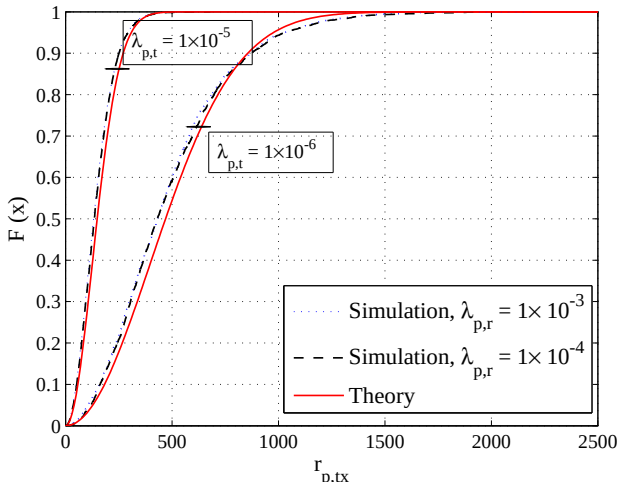

Fig. 2: The theoretical and simulated CDF of $r_{p,tx}$ under different PU transmitter and receiver densities.

B. Interference form the underlay network

In addition to the interference from the primary network, a given CU receiver will experience interference from other unassociated CU transmitters. We will now consider this interference I_u.

As mentioned in Section II, because CU nodes must not transmit whenever they are within the guard region of a PU receiver, the active CU transmitters actually form a Poisson hole process [15], which is defined as follows. When Φ_A and Φ_B are independent homogeneous PPPs, and $\forall x \in \Phi_A$, points from Φ_B are removed within a radius b from x, the remaining points of Φ_B form a Poisson hole process [15]. However, the Poisson hole processes is not mathematically tractable, and its probability generating functional is not known [15]. Instead, we can approximate the active CU transmitters as an independently thinned PPP using the coloring theorem [46]. If $\bar{\lambda}_{u,t}$ is the density of the active CU transmitters, it can be written as $\bar{\lambda}_{u,t} = \delta\lambda_{u,t}$, where δ is the probability that any particular transmitter doesn't fall within the guard region of a PU receiver. Using the void probability, δ is obtained as $\delta = e^{-\pi\lambda_{p,r}R_G^2}$, and $\bar{\lambda}_{u,t} = \lambda_{u,t}e^{-\pi\lambda_{p,r}R_G^2}$. However, recent research has established tight bounds for the interference from Poisson hole processes which performs better than the independent thinning approximation [50]. But, the mathematical tractability is less.

We will now derive the MGF of I_u for the two different system models for the underlay network.

1) voronoi model: When the voronoi model is considered for the underlay network, we will consider two cases of association where : 1) the receiver selects the closest transmitter, and 2) the transmitter initiates communication and selects the closest receiver. The first scheme is more prevalent in traditional mobile networks for the downlink and wireless LAN while the second scheme is more suitable for ad-hoc and sensor networks.

- *Receiver selects the closest transmitter*
  In this scheme, a receiver selects the closest transmitter to associate. Let the available CU transmitters be denoted as the PPP $\bar{\Phi}_{u,t}$. If the receiver is connected to the CU transmitter $z \in \bar{\Phi}_{u,t}$, the total interference from the underlay network is written as $I_u = \sum_{i\in\bar{\Phi}_{u,t}\setminus z} I_{u,i}$, where $I_{u,i}$ is the interference from the i-th CU transmitter. $I_{u,i}$ is written as $I_{u,i} = \mathcal{B}P_s|h|^2 r_s^{-\alpha}$, where P_s is the transmit power of a CU transmitter defined as $P_s = P_u r_{u,tx}^{\alpha}$ and $r_{u,tx}$ is the distance between a CU transmitter and the associated receiver. r_s is the distance from an interfering CU transmitter to the CU receiver in question, and $\mathcal{B}$ is a Bernoulli random variable taking on the value 1 when $r_{u,tx} < D$, and 0 otherwise.
  Using the same technique used to obtain the distribution of $r_{p,tx}$, the distribution of $r_{u,tx}$ can be shown to have the approximate PDF $Ral(\pi\bar{\lambda}_{u,t})$. Let β be the probability that $r_{u,tx} < D$. Then, $\beta = 1 - e^{-\pi\bar{\lambda}_{u,t}D^2}$.
  Using the Campbell's theorem, we can write $M_{I_u}(s)$ as
  $$M_{I_u}(s) = e^{\left(\int_r^{\infty} \mathbb{E}_{r_{u,tx}}\left[1-\beta+\frac{\beta}{1+sP_u r_{u,tx}^{\alpha} r_s^{-\alpha}}-1\right] 2\pi\bar{\lambda}_{u,t} r_s dr_s\right)} \quad (7)$$
  where $r(< D)$ is the distance between the receiver in question and the associated transmitter. For any given associated receiver, r is deterministic. A closed-form solution for (7) is not apparent, and can be solved using numerical techniques. A simplified equation for $M_{I_u}(s)$ obtained after some manipulations and a series expansion when $sP_u r_{u,tx}^{\alpha} r_s^{-\alpha} < 1$ as (8). This method works when $s << \frac{1}{P_u}$, and this condition is satisfied for practical system parameters. Furthermore, the mean interference $\mathbb{E}[I_u]$ can be derived as (9).
  For the special case when we do not take r to be deterministic, we need the distribution of r. It is obtained by conditioning the distance distribution from any CU receiver to its active closest CU transmitter (given as $Ral(\pi\bar{\lambda}_{u,t})$) by the condition that the maximum allowable distance is D (the distance from any CU receiver to its active closest CU transmitter should not exceed D, and this event occurs with a probability of $1-e^{-\pi\bar{\lambda}_{u,t}D^2}$). As such, we can write $f_r(x) = \frac{Ral(\pi\bar{\lambda}_{u,t})}{1-e^{-\pi\bar{\lambda}_{u,t}D^2}}$, which is expressed for notational simplicity as $TRal(\pi\bar{\lambda}_{u,t}, D)$. Therefore, if (8) is written as $M_{I_u}(s) = e^{\mathcal{W}}$, $M_{I_u}(s)$ for non-deterministic r becomes $M_{I_u}(s) = e^{\mathbb{E}_r[\mathcal{W}]}$. However, $\mathbb{E}_r[\mathcal{W}]$ does not necessarily converge for $k > 1$. But, when $sP_u << 1$ and $\alpha < 4$, the summation in (8) can be accurately approximated by the first term. As such, the MGF can be written as (10).
- *Transmitter selects the closest receiver*
  Here, the association attempt is initiated by the CU transmitter corresponding to a situation where those nodes are the data generators. Within this scheme, an available CU transmitter ($\in \bar{\Phi}_{u,t}$) selects the nearest CU receiver to associate with.
  Let the CU receiver for which performance is analyzed be connected to the CU transmitter $z \in \bar{\Phi}_{u,t}$. The total interference from the underlay network is written similar to the previous scheme as $I_u = \sum_{i\in\bar{\Phi}_{u,t}\setminus z} I_{u,i}$. $I_{u,i}$ is written as $I_{u,i} = \mathcal{C}P_s|h|^2 r_s^{-\alpha}$, where P_s is the transmit power of a CU transmitter defined as $P_s = P_u r_{s,rx}^{\alpha}$. $r_{s,rx}$ is the distance between a CU transmitter and the closest

$$M_{I_u}(s) = \approx e^{\left(2\pi\bar{\lambda}_{u,t}\sum_{k=1}^{\infty}\frac{(-sP_u)^k}{(\alpha k-2)(\pi\bar{\lambda}_{u,t})^{\frac{\alpha k}{2}}}r^{2-\alpha k}\left(\Gamma\left(\frac{\alpha k}{2}+1\right)-\Gamma\left(\frac{\alpha k}{2}+1,\pi\bar{\lambda}_{u,t}D^2\right)\right)\right)}, sP_u << 1 \quad (8)$$

$$\mathbb{E}[I_u] \approx \frac{(2\pi\bar{\lambda}_{u,t}P_u}{(\alpha-2)(\pi\bar{\lambda}_{u,t})^{\frac{\alpha}{2}}}r^{2-\alpha}\left(\Gamma\left(\frac{\alpha}{2}+1\right)-\Gamma\left(\frac{\alpha}{2}+1,\pi\bar{\lambda}_{u,t}D^2\right)\right), sP_u << 1 \quad (9)$$

$$M_{I_u}(s) \approx e^{\left(\frac{-2sP_u}{(\alpha-2)(1-e^{-\pi\bar{\lambda}_{u,t}D^2})}\left(\Gamma\left(\frac{\alpha}{2}+1\right)-\Gamma\left(\frac{\alpha}{2}+1,\pi\bar{\lambda}_{u,t}D^2\right)\right)\left(\Gamma\left(2-\frac{\alpha}{2}\right)-\Gamma\left(2-\frac{\alpha}{2},\pi\bar{\lambda}_{u,t}D^2\right)\right)\right)}, sP_u << 1, \alpha < 4 \quad (10)$$

receiver and $\mathcal{C}$ is a Bernoulli random variable taking on the value 1 when $r_{s,rx} < D$, and 0 otherwise. Using the void probability of a PPP [46], the distance $r_{s,rx}$ can be shown to have the PDF $Ral(\pi\lambda_{s,r})$. Let ζ be the probability that $r_{s,rx} < D$. Then, $\zeta = 1 - e^{-\pi\lambda_{s,r}D^2}$.

Unlike the previous scheme, a complication arises when evaluating the MGF of I_u. Although a transmitter selects its closest receiver node, from the point of the CU receiver for which performance is evaluated, transmitter z is not the closest transmitter in general. As such, we will approximate I_u as $I_u \approx \sum_{i\in\bar{\Phi}_{u,t}} I_{u,i}$. In effect, our approximation gives an upper bound on the interference and thus the outage.

With the Campbell's theorem, the MGF of the interference from underlay nodes $M_{I_u}(s)$ is written as $M_{I_u}(s) \approx e^{\left(\int_0^\infty \mathbb{E}_{r_{s,rx}}\left[1-\zeta+\frac{\zeta}{1+sP_u r_{s,rx}^{\alpha} r_s^{-\alpha}}-1\right]2\pi\bar{\lambda}_{u,t}r_s dr_s\right)}$. When $\alpha > 2$, the MGF becomes

$$M_{I_u}(s) \approx e^{\left(-\frac{2\pi\bar{\lambda}_{u,t}e^{-\pi\lambda_{s,r}D^2}}{\alpha\lambda_{s,r}}\frac{(sP_u)^{\frac{2}{\alpha}}}{\sin\left(\frac{2\pi}{\alpha}\right)}\left(e^{\pi\lambda_{s,r}D^2}-\pi\lambda_{s,r}D^2-1\right)\right)} \quad (11)$$

The mean interference $\mathbb{E}[I_u]$ does not converge while using the simplified path loss model, and thus we will use $g(r_s) = \min(1, r_s^{-\alpha})$. Using this, $E[I_u]$ can be obtained as

$$\mathbb{E}[I_u] = \frac{\pi\alpha\bar{\lambda}_{u,t}P_u}{(\alpha-2)(\pi\lambda_{s,r})^{\frac{\alpha}{2}}}\left(\Gamma\left(\frac{\alpha}{2}+1\right)-\Gamma\left(\frac{\alpha}{2}+1,\pi\lambda_{s,r}D^2\right)\right) \quad (12)$$

2) Cluster model: Here, each CU receiver associates with its cluster head. We assume that all cluster heads (CU transmitters) outside the guard regions of PU receivers are available for association, and thus potentially active (with a density of $\bar{\lambda}_{u,t}$). If this assumption is not true, our analysis yields a worst-case performance benchmark. Let these available CU transmitters be denoted by the Poisson point process $\bar{\Phi}_{u,t}$, and the particular receiver node whose performance is analyzed is connected with the z-th cluster head where $z \in \bar{\Phi}_{u,t}$. The interference from CU transmitters I_u is written as $I_u = \sum_{i\in\bar{\Phi}_{u,t}\setminus z} I_{u,i}$, where the interference from the i-th CU transmitter is given by $I_{u,i} = P_s|h|^2 r_{sc}^{-\alpha}$. P_s is the transmit power of a CU transmitter, and r_{sc} and $|h|^2$ are the distance and channel power gain between an underlay cluster head, and the CU receiver whose performance is analyzed. The transmit power of the CU transmitter is given by $P_s = P_u r_{c,tx}^{\alpha}$, where $r_{c,tx}$ is the distance between the i-th CU transmitter and its associated receiver. Due to the CU receivers within a cluster forming a homogeneous PPP, they are uniformly distributed spatially. Therefore, the CDF of $r_{c,tx}$ can be obtained by considering the number of nodes within a distance x from the i-th CU transmitter as [51]

$$F_{r_{c,tx}}(x) = \frac{x^2}{\left(\frac{d_l}{2}\right)^2}, 0 < x < \frac{d_l}{2}. \quad (13)$$

Thus, the PDF of $r_{c,tx}$ is simply obtained by differentiating (13), and is expressed as $f_{r_{c,tx}}(x) = \frac{2x}{(d_l 2)^2}, 0 < x < \frac{d_l}{2}$, which is $Lin(\frac{d_l}{2})$.

Even though all CU transmitters outside guard regions should be active, if a CU receiver requiring association does not exist, the given CU transmitter remains inactive. Let ρ be the probability that the cluster head is actually associated with a receiver. Thus ρ is the probability that at least a single CU receiver exists within the cluster given by $\rho = 1 - e^{-\pi\lambda_{u,r}\left(\frac{d_l}{2}\right)^2}$. By using independent thinning [46], the density of active CU transmitters is obtained as $\rho\bar{\lambda}_{u,t}$. Moreover, for a given receiver, its cluster head may or may not be the closest transmitter, which is especially true for the receivers towards the cluster's edge. This is because different clusters may spatially overlap. Now, using Slivnyak's theorem [11], [40], the interfering underlay base stations may be approximated as a homogeneous PPP.

Therefore, using the Campbell's theorem, $M_{I_u}(s)$ can be written as

$$M_{I_u}(s) = e^{\left(\int_0^\infty \mathbb{E}_{r_{c,tx}}\left[\frac{1}{1+sP_u r_{c,tx}^{\alpha} r_{sc}^{-\alpha}}-1\right]2\pi\rho\bar{\lambda}_{u,t}r_{sc}dr_{sc}\right)}. \quad (14)$$

When $\alpha > 2$, we obtain a closed form expression for $M_{I_u}(s)$ as

$$M_{I_u}(s) = e^{\left(-\frac{2\pi^2\rho\bar{\lambda}_{u,t}}{\alpha}\frac{(sP_u)^{\frac{2}{\alpha}}}{\sin\left(\frac{2\pi}{\alpha}\right)}\mathbb{E}\left[r_{c,tx}^2\right]\right)} = e^{\left(-\frac{\pi^2\rho\bar{\lambda}_{u,t}}{\alpha}\frac{(sP_u)^{\frac{2}{\alpha}}\left(\frac{d_l}{2}\right)^2}{\sin\left(\frac{2\pi}{\alpha}\right)}\right)}. \quad (15)$$

Using $g(r) = \min(1, r_{sc}^{-\alpha})$, we find the mean interference $\mathbb{E}[I_u]$ to be

$$\mathbb{E}[I_u] = \int_0^\infty \mathbb{E}_{|h|^2, r_{c,tx}}[P_u|h|^2 r_{c,tx}^{\alpha} r_{sc}^{-\alpha}]2\pi\rho\bar{\lambda}_{u,t}r_{sc}dr_{sc} = \frac{2\pi\rho P_u\bar{\lambda}_{u,t}\alpha\left(\frac{d_l}{2}\right)^2}{(\alpha-2)(\alpha+2)}. \quad (16)$$

IV. Outage analysis with massive MIMO enabled base stations

A. Channel estimation

Both primary and underlay base stations estimate the downlink channel, via an initial uplink training phase. During which, the PU and CU receivers transmit pilot sequences to their serving base stations.

1) Primary system: We now consider the set of pilot signals using the a-th ($a \in \{1, ...q\}$) pilot sequence arriving at a primary base station. However, only a subsection of the primary and underlay base stations will use the a-th pilot sequence. As such, those active primary and underlay base stations are denoted by $\bar{\Phi}_{p,t}$ and $\bar{\Phi}_{u,t}$ respectively. Let $\phi_{pr,la}$ and $\phi_{ur,wa}$ respectively be the PU receiver using the a-th pilot sequence connected to $\bar{\phi}_{p,t,l}$ and the CU receiver using the a-th pilot sequence connected to $\bar{\phi}_{u,t,w}$, where $\bar{\phi}_{p,t,l}$ is the l-th

PU transmitter $\in \bar{\Phi}_{p,t}$ and $\bar{\phi}_{u,t,w}$ is the w-th CU transmitter $\in \bar{\Phi}_{u,t}$.

The received signal y_k at the k-th primary base station ($\bar{\phi}_{p,t,k} \in \bar{\Phi}_{p,t}$) will be comprised of all pilot signals using different pilot sequences from all associated PU receivers and CU receivers. However, as orthogonal pilots are used, we restrict our attention to the signals containing the a-th pilot sequence without the loss of generality. Let $\bar{y}_{ka}$ denote the received signal corresponding to the a-th pilot sequence. Then, $\bar{y}_k$ is written as

$$\bar{y}_{ka} = \sum_{l=1}^{\infty} \mathbf{h}_{kla} r_{kla}^{\frac{-\alpha}{2}} b_a^T \sqrt{P_{p,p}} r_{la}^{\frac{\alpha}{2}} + \sum_{w=1}^{\infty} \mathbf{h}_{kwa} r_{kwa}^{\frac{-\alpha}{2}} b_a^T \sqrt{P_{p,u}} r_{wa}^{\frac{\alpha}{2}} + \mathbf{w}_k, \quad (17)$$

where $\mathbf{h}_{kla}$ and r_{kla} are the channel gain and distance between $\bar{\phi}_{p,t,k}$ and $\phi_{pr,la}$, $\mathbf{h}_{kwa}$ and r_{kwa} are the channel gain and distance between $\bar{\phi}_{p,t,k}$ and $\phi_{ur,wa}$, r_{la} is the distance between $\phi_{pr,la}$ and $\bar{\phi}_{p,t,l}$, r_{wa} is the distance between $\phi_{ur,wa}$ and $\bar{\phi}_{u,t,w}$, and $\mathbf{w}_k$ is the received noise. The received signal $\bar{y}_{ka} \in \mathbb{C}^{M \times L}$, $\mathbf{w}_k \in \mathbb{C}^{M \times L}$, and $\mathbf{h}_{kla}, \mathbf{h}_{kwa} \in \mathbb{C}^{M \times 1}$.

The objective of $\bar{\phi}_{p,t,k}$ is to estimate the channel gain between it and $\phi_{pr,ka}$, where $\phi_{pr,ka} \in \Phi_{p,r}$ is the PU receiver using the a-th pilot sequence associated with $\bar{\phi}_{p,t,k}$. If this channel gain is denoted as $\mathbf{h}_{kka}$, the estimated channel gain $\hat{\mathbf{h}}_{kka}$ may be expressed as

$$\begin{aligned} \hat{\mathbf{h}}_{kka} &= \frac{\bar{y}_{ka} b_a}{\sqrt{P_{p,p}}} \\ &= \mathbf{h}_{kka} + \sum_{l=1\backslash k}^{\infty} \mathbf{h}_{kla} r_{kla}^{\frac{-\alpha}{2}} r_{la}^{\frac{\alpha}{2}} + \sum_{w=1}^{\infty} \mathbf{h}_{kwa} r_{kwa}^{\frac{-\alpha}{2}} \sqrt{\frac{P_{p,u}}{P_{p,p}}} r_{wa}^{\frac{\alpha}{2}} + \frac{\mathbf{w}_k b_a}{\sqrt{P_{p,p}}} \end{aligned} \quad (18)$$

2) Underlay system: Within this subsection, we derive the estimated channel gain between the z-th underlay base station $\bar{\phi}_{u,t,z} \in \bar{\Phi}_{u,t}$ and its associated CU receiver using the a-th pilot sequence $\phi_{ur,za}$. If $\bar{y}_{za} \in \mathbb{C}^{N \times L}$ is the received signal at $\bar{\phi}_{u,t,z}$ corresponding to the a-th pilot sequence,

$$\begin{aligned} \bar{y}_{za} = &\sum_{l=1}^{\infty} \mathbf{h}_{zla} r_{zla}^{\frac{-\alpha}{2}} b_a^T \sqrt{P_{p,p}} r_{la}^{\frac{\alpha}{2}} \\ &+ \sum_{w=1}^{\infty} \mathbf{h}_{zwa} r_{zwa}^{\frac{-\alpha}{2}} b_a^T \sqrt{P_{p,u}} r_{wa}^{\frac{\alpha}{2}} + \mathbf{w}_z, \end{aligned} \quad (19)$$

where the notation is analogous to the previous subsection. The estimated channel gain $\mathbf{h}_{zza}$ is obtained in a similar way to (18) as

$$\begin{aligned} \hat{\mathbf{h}}_{zza} &= \frac{\bar{y}_{za} b_a}{\sqrt{P_{p,u}}} \\ &= \mathbf{h}_{zza} + \sum_{w=1\backslash z}^{\infty} \mathbf{h}_{zwa} r_{zwa}^{\frac{-\alpha}{2}} r_{wa}^{\frac{\alpha}{2}} + \sum_{l=1}^{\infty} \mathbf{h}_{zla} r_{zla}^{\frac{-\alpha}{2}} \sqrt{\frac{P_{p,p}}{P_{p,u}}} r_{la}^{\frac{\alpha}{2}} + \frac{\mathbf{w}_z b_a}{\sqrt{P_{p,u}}} \end{aligned} \quad (20)$$

B. Downlink transmission

1) Interference from PU transmitters: A PU transmitter will estimate the channel and then transmit the data symbols to its associated receivers in the downlink. The downlink transmissions to the receivers using the a-th pilot sequence occurs simultaneously. That is, the base stations operate synchronously. This assumption allows us to characterize the maximum level of interference due to pilot contamination.

Each base station $\bar{\phi}_{p,t,j} \in \bar{\Phi}_{p,t}$ uses a precoding scheme where the transmit symbol to $\phi_{pr,ja}$ is precoded with the estimated channel gain $\hat{\mathbf{h}}_{jja}$. This process occurs for all associated receivers, and the summation of the precoded signals are transmitted [11].

Our objective is to obtain the received signal at a typical CU receiver utilizing the a-th pilot signal. Let $\phi_{ur,za}$ denote this node which is associated with the z-th underlay base station $\bar{\phi}_{u,t,z}$. The received interference from primary base stations at $\phi_{ur,za}$ is written as

$$Y_{za,p} = \sum_{j=1}^{\infty} \mathbf{h}_{jza}^* r_{jza}^{\frac{-\alpha}{2}} x_j, \quad (21)$$

where $\mathbf{h}_{jza}^*$ and $r_{jza}^{\frac{-\alpha}{2}}$ are the channel gain and path loss between $\bar{\phi}_{p,t,j}$ and $\phi_{ur,za}$, and x_j is the transmit symbol by $\bar{\phi}_{p,t,j}$. $\mathbf{h}_{jza}^*$ is the reciprocal of the channel gain between $\phi_{ur,za}$ and $\bar{\phi}_{p,t,j}$ because a TDD system is considered. The transmitted symbol x_j is expressed as

$$x_j = \sum_{\nu=1}^{q_j} \hat{\mathbf{h}}_{jj\nu} \sqrt{\frac{P_p}{M}} r_{jj\nu}^{\frac{\alpha}{2}} d_{j\nu}, \quad (22)$$

where $q_j (< q)$ is the number of associated PU receivers of $\bar{\phi}_{p,t,j}$, $\hat{\mathbf{h}}_{jj\nu}$ and $r_{jj\nu}$ are the estimated uplink channel and distance between $\bar{\phi}_{p,t,j}$ and $\phi_{pr,j\nu}$, and $d_{j\nu}$ is the data symbol intended for $\phi_{pr,j\nu}$. After scaling $Y_{za,p}$ with respect to $\sqrt{M}$, the received interference from primary base stations is written as

$$\begin{aligned} \tilde{Y}_{za,p} &= \lim_{M \to \infty} \frac{Y_{za,p}}{\sqrt{M}} \\ &= \lim_{M \to \infty} \frac{1}{M} \sum_{j=1}^{\infty} \mathbf{h}_{jza}^* r_{jza}^{\frac{-\alpha}{2}} \sqrt{P_p} \sum_{\nu=1}^{q_j} r_{jj\nu}^{\frac{\alpha}{2}} d_{j\nu} \times \\ &\left(\mathbf{h}_{jj\nu} + \sum_{l=1\backslash j}^{\infty} \mathbf{h}_{jl\nu} r_{jl\nu}^{\frac{-\alpha}{2}} r_{l\nu}^{\frac{\alpha}{2}} + \sum_{w=1}^{\infty} \mathbf{h}_{jw\nu} r_{jw\nu}^{\frac{-\alpha}{2}} \sqrt{\frac{P_{p,u}}{P_{p,p}}} r_{w\nu}^{\frac{\alpha}{2}} + \frac{\mathbf{w}_j b_\nu}{\sqrt{P_{p,p}}} \right) \end{aligned} \quad (23)$$

However, $\lim_{M \to \infty} \frac{\mathbf{h}_{jza}^* \mathbf{h}_{jl\nu}}{M} \to 0, \forall j, \nu, l$ because independent and identically distributed channel gains are considered for different links, and $\lim_{M \to \infty} \frac{\mathbf{h}_{jza}^* \mathbf{w}_j b_\nu}{M} \to 0$, $\forall j$. Furthermore, $\lim_{M \to \infty} \frac{\mathbf{h}_{jza}^* \mathbf{h}_{jw\nu}}{M} \to 1$ whenever $w = z, \nu = a$. Thus, $\tilde{Y}_{za,p}$ can be expressed as

$$\tilde{Y_{za,p}} = \sum_{j=1}^{\infty} \sqrt{\frac{P_p P_{p,u}}{P_{p,p}}} r_{jza}^{-\alpha} r_{jja}^{\frac{\alpha}{2}} r_{za}^{\frac{\alpha}{2}} d_{ja}. \quad (24)$$

2) Downlink signal from CU transmitters: Similar to the downlink transmission from primary base stations, each underlay base station $\bar{\phi}_{u,t,i} \in \bar{\Phi}_{u,t}$ precodes its symbol to $\phi_{ur,ia}$ with the estimated channel gain $\hat{h}_{iia}$. We will assume that downlink transmissions from all CU transmitters occur at the same time. The received signal from underlay base stations at $\phi_{ur,za}$ is thus written as

$$Y_{za,u} = \sum_{i=1}^{\infty} \mathbf{h}_{iza}^* r_{iza}^{\frac{-\alpha}{2}} x_i, \quad (25)$$

where x_i is defined by

$$x_j = \sum_{\nu=1}^{q_i} \hat{\mathbf{h}}_{ii\nu} \sqrt{\frac{P_u}{N}} r_{ii\nu}^{\frac{\alpha}{2}} d_{i\nu}. \tag{26}$$

The number of associated CU receivers of $\bar{\phi}_{u,t,i}$ is denoted by $q_i (< q)$. After scaling $Y_{za,u}$ with respect to $\sqrt{M}$, the signal from the underlay base stations is written as

$$\begin{aligned}
\tilde{Y}_{za,u} &= \lim_{M\to\infty} \frac{Y_{za,u}}{\sqrt{M}} \\
&= \lim_{N\to\infty} \frac{1}{\sqrt{\kappa} N} \sum_{i=1}^{\infty} \mathbf{h}_{iza}^{*} r_{iza}^{\frac{-\alpha}{2}} \sqrt{P_u} \sum_{\nu=1}^{q_i} r_{ii\nu}^{\frac{\alpha}{2}} d_{i\nu} \times \\
&\left(\mathbf{h}_{ii\nu} + \sum_{w=1\setminus i}^{\infty} \mathbf{h}_{iw\nu} r_{iw\nu}^{\frac{-\alpha}{2}} r_{w\nu}^{\frac{\alpha}{2}} + \sum_{l=1}^{\infty} \mathbf{h}_{il\nu} r_{il\nu}^{\frac{-\alpha}{2}} \sqrt{\frac{P_{p,p}}{P_{p,u}}} r_{l\nu}^{\frac{\alpha}{2}} + \frac{\mathbf{w}_i b_\nu}{\sqrt{P_{p,u}}} \right) \\
&= \frac{\sqrt{P_u}}{\sqrt{\kappa}} + \sum_{i=1\setminus z}^{\infty} \frac{\sqrt{P_u}}{\sqrt{\kappa}} r_{iza}^{-\alpha} r_{iia}^{\frac{\alpha}{2}} r_{za}^{\frac{\alpha}{2}} d_{ia}.
\end{aligned} \tag{27}$$

The first term of (27) represents the desired signal to $\phi_{ur,za}$ while the second term represents the interference from CU transmitters.

3) Interfering base station density: In the previous subsections, we expressed the interference to $\phi_{ur,za}$ from primary and CU transmitters using the a-th pilot sequence (namely $\bar{\Phi}_{p,t}$ and $\bar{\Phi}_{u,t}$). This subsection derives the densities of these processes.

- *Density of* $\bar{\Phi}_{p,t}$
  We will first derive the density of density of $\bar{\Phi}_{p,t}$ denoted as $\bar{\lambda}_{p,t}$. To this end, we approximate $\bar{\Phi}_{p,t}$ as a thinned PPP [46] where the density $\bar{\lambda}_{p,t} = \eta \lambda_{p,t}$. The factor η is the probability that a particular base station uses the a-th ($a \in \{1, ...q\}$) pilot sequence.
  We will consider a typical primary base station $\phi_{p,t,k} \in \Phi_{p,t}$. The number of users associated with $\phi_{p,t,k}$ is a random variable depending on the area of its Voronoi cell (S). However, the exact distribution of the area of a Voronoi cell is not known. Consequently, a two parameter gamma empirical approximation [52] has been shown to fit the exact size distribution. Thus, the normalized cell size $\tilde{S} = S/\bar{S}$ is distributed as follows:

$$f_{\tilde{S}}(y) \approx \frac{\beta^\mu}{\Gamma(\mu)} y^{\mu-1} e^{-\beta y}, 0 \le y < \infty, \tag{28}$$

  where $\mu = 3.61$, $\beta = 3.57$, and $\bar{S}$ is the average size of a cell given by $\bar{S} = \frac{1}{\lambda_{p,t}}$.
  Let ω_1 be the number of associated users with $\phi_{p,t,k}$. When $\omega_1 \ge q$, all the pilot sequences will be used whereas when $\omega_1 < q$ there exists a probability that the a-th pilot sequence is not used by any user associated with $\phi_{p,t,k}$. Thus, we can write η as

$$\begin{aligned}
\eta &= \Pr[\omega_1 \ge q] + \Pr[\omega_1 < q] \frac{\mathbb{E}_{\omega_1 \setminus \omega_1 < q}[\omega_1]}{q} \\
&= \mathbb{E}_S \left[\sum_{n=q}^{\infty} \frac{(\lambda_{p,r} S)^n}{n!} e^{-\lambda_{p,r} S} + \frac{1}{q} \sum_{\omega_1=1}^{q-1} \frac{(\lambda_{p,r} S)^{\omega_1}}{\omega_1 - 1!} e^{-\lambda_{p,r} S} \right]
\end{aligned} \tag{29}$$

  Substituting $S = \tilde{S}\bar{S}$ and performing the expectation with respect to (28) we obtain

$$\begin{aligned}
\eta &= \frac{\beta^\mu}{\Gamma(\mu)} \sum_{n=q}^{\infty} \frac{\Gamma(\mu+n)}{n! (\beta + \frac{\lambda_{p,r}}{\lambda_{p,t}})^{\mu+n}} \left(\frac{\lambda_{p,r}}{\lambda_{p,t}} \right)^n \\
&+ \frac{1}{q} \frac{\beta^\mu}{\Gamma(\mu)} \sum_{\omega_1=1}^{q-1} \frac{\Gamma(\mu+\omega_1)}{(\omega_1 - 1)! (\beta + \frac{\lambda_{p,r}}{\lambda_{p,t}})^{\mu+\omega_1}} \left(\frac{\lambda_{p,r}}{\lambda_{p,t}} \right)^{\omega_1}
\end{aligned} \tag{30}$$

- *Density of* $\bar{\Phi}_{u,t}$ for the cluster model
  We now derive the density of $\bar{\Phi}_{u,t}$ for the cluster model denoted as $\bar{\lambda}_{u,t}$. Similar to before, $\bar{\Phi}_{u,t}$ can be obtained by applying independent thinning on $\Phi_{u,t}$. Therefore, $\bar{\lambda}_{u,t} = \theta \hat{\lambda}_{u,t}$, and θ is the probability that a particular underlay base station uses the a-th pilot sequence while $\hat{\lambda}_{u,t}$ is given by $\hat{\lambda}_{u,t} = \tilde{\theta} \lambda_{u,t}$, where $\tilde{\theta}$ is the probability that a CU transmitter is not inside the guard region of a PU receiver given by $\tilde{\theta} = e^{-\pi \lambda_{p,r} R_G^2}$.
  Let $\phi_{u,t,z} \in \Phi_{u,t}$ be a typical active CU transmitter. Although the cluster area of $\phi_{u,t,z}$ is fixed, the number of receivers associated with it (ω_2) is still a random variable. We can thus write θ as

$$\begin{aligned}
\theta &= \Pr[\omega_2 > q] + \Pr[\omega_2 < q] \frac{\mathbb{E}_{\omega_2 \setminus \omega_2 < q}[\omega_2]}{q} \\
&= \sum_{n=q}^{\infty} \frac{(\lambda_{u,r} \frac{\pi d_l^2}{4})^n}{n!} e^{-\lambda_{u,r} \frac{\pi d_l^2}{4}} \\
&+ \frac{1}{q} \sum_{\omega_2=1}^{q-1} \frac{(\lambda_{u,r} \frac{\pi d_l^2}{4})^{\omega_2}}{\omega_2 - 1!} e^{-\lambda_{u,r} \frac{\pi d_l^2}{4}}.
\end{aligned} \tag{31}$$

- *Density of* $\bar{\Phi}_{u,t}$ for the voronoi model
  The density of $\bar{\Phi}_{u,t}$ for the voronoi model (denoted as $\bar{\lambda}_{u,t}$) is written similar to the cluster model as $\bar{\lambda}_{u,t} = \theta \hat{\lambda}_{u,t}$, where $\hat{\lambda}_{u,t} = \tilde{\theta} \lambda_{u,t}$ and $\tilde{\theta} = e^{-\pi \lambda_{p,r} R_G^2}$. However, θ is analogous to η and is written as

$$\begin{aligned}
\theta &= \frac{\beta^\mu}{\Gamma(\mu)} \sum_{n=q}^{\infty} \frac{\Gamma(\mu+n)}{n! (\beta + \frac{\lambda_{u,r}}{\hat{\lambda}_{u,t}})^{\mu+n}} \left(\frac{\lambda_{u,r}}{\hat{\lambda}_{u,t}} \right)^n \\
&+ \frac{1}{q} \frac{\beta^\mu}{\Gamma(\mu)} \sum_{\omega_1=1}^{q-1} \frac{\Gamma(\mu+\omega_1)}{(\omega_1 - 1)! (\beta + \frac{\lambda_{u,r}}{\hat{\lambda}_{u,t}})^{\mu+\omega_1}} \left(\frac{\lambda_{u,r}}{\hat{\lambda}_{u,t}} \right)^{\omega_1}
\end{aligned} \tag{32}$$

C. Interference characterization

We now characterize the interference at $\phi_{ur,za}$ and obtain the outage probability. The aggregate interference scaled with respect to $\sqrt{M}$ (I) can be written as $I = I_p + I_u$, where $I_p = \sum_{j=1}^{\infty} \frac{P_p P_{p,u}}{P_{p,p}} r_{jza}^{-2\alpha} r_{jja}^{\alpha} r_{za}^{\alpha}$ and $I_u = \sum_{i=1\setminus z}^{\infty} \frac{P_u}{\kappa} r_{iza}^{-2\alpha} r_{iia}^{\alpha} r_{za}^{\alpha}$. Without the loss of generality, we assume that $d_{ja}^2, d_{ia}^2 = 1$. The SIR[5] (γ) at $\phi_{ur,za}$ is written as $\gamma = \frac{P_u}{\kappa(I_p + I_u)}$, and the outage probability is expressed as

$$P_O = \Pr[\gamma < T] = \Pr[I > \frac{P_u}{\kappa T}], \tag{33}$$

where T is the threshold SIR required at a CU receiver. In order to evaluate P_O, the distribution of I is required.

[5]Note that SIR is equal to the SINR (signal to interference and noise ratio) because the noise power approaches zero when scaled by $\sqrt{M}$.

To this end, we will first evaluate the MGF of I. However, because I_p and I_u are independent, $M_I(s)$ becomes $M_I(s) = \mathbb{E}[e^{-sI_p}]\mathbb{E}[e^{-sI_u}] = M_{I_p}(s)M_{I_u}(s)$. Using the Campbell's theorem [46], M_{I_p} is expressed as

$$M_{I_p}(s)=e^{\left(\int_0^\infty \mathbb{E}\left[e^{-s\frac{P_pP_{p,u}}{P_{p,p}}r_{jza}^{-2\alpha}r_{jja}^{\alpha}r_{za}^{\alpha}}-1\right]2\pi\bar{\lambda}_{p,t}r_{jza}dr_{jza}\right)}, \quad (34)$$

where the expectation is with respect to r_{jja} and r_{za}. Therefore, in order to evaluate (34), the distributions of r_{jja} and r_{za} are needed.

1) Cluster model: The variable r_{jja} can be interpreted as the distance from a primary base station to any associated receiver. However, the receiver can be located at any point within the Voronoi cell of $\bar{\phi}_{p,t,j}$. It has been shown in [53] that r_{jja} has the approximate PDF given by $Ral(\pi\lambda_{p,t})$. However, it is worth emphasizing that this is not the exact PDF due to correlations and dependence induced by the structure of the Voronoi tessellation. On the contrary, r_{za} which can be interpreted as the distance between a cluster head and a random daughter node in the cluster has an exact simple PDF given by $Lin(\frac{d_l}{2})$.

Using the PDFs for r_{za} and r_{jja}, and replacing r_{jza} with r for clarity, we can simplify (34) as

$$M_{I_p}(s)=e^{\left(\int_0^\infty \mathbb{E}_{r_{jja},r_{za}}\left[\sum_{v=1}^\infty \frac{\left(-s\frac{P_pP_{p,u}}{P_{p,p}}r^{-2\alpha}r_{jja}^{\alpha}r_{za}^{\alpha}\right)^v}{v!}\right]2\pi\bar{\lambda}_{pt}rdr\right)}$$
$$=e^{\left(\sum_{v=1}^\infty \frac{\pi\bar{\lambda}_{pt}}{v!}\left(\frac{-sP_pP_{p,u}}{P_{p,p}}\right)^v\left(\frac{\alpha v d_l^{\alpha v}\Gamma(\frac{\alpha v}{2}+1)}{(\alpha v-1)2^{\alpha v-1}(\alpha v+2)(\pi\lambda_{p,t})^{\frac{\alpha v}{2}}}\right)\right)}, \quad (35)$$

From (35), it is possible to obtain the first and second order statistics of I_p[6] as $\mathbb{E}[I_p] = \frac{\eta P_pP_{p,u}\alpha d_l^{\alpha}\Gamma(\frac{\alpha}{2}+1)}{P_{p,p}(\alpha-1)2^{\alpha-1}(\alpha+2)(\pi\lambda_{p,t})^{\frac{\alpha}{2}-1}}$ and $Var[I_p] = \frac{\eta(P_pP_{p,u})^2\alpha d_l^{2\alpha}\Gamma(\alpha+1)}{P_{p,p}^2(2\alpha-1)2^{2\alpha-1}(\alpha+1)(\pi\lambda_{p,t})^{\alpha-1}}$.

We now focus our attention I_u. Using the Slivnyak's theorem [11], [40], the interfering underlay base stations ($\bar{\Phi}_{u,t}\backslash z$) can be taken as forming a homogeneous PPP. Therefore, using Campbell's theorem [46], $M_{I_u}(s)$ is written as

$$M_{I_u}(s) = e^{\left(\int_0^\infty \mathbb{E}\left[e^{-s\frac{P_u}{\kappa}r_{iza}^{-2\alpha}r_{iia}^{\alpha}r_{za}^{\alpha}}-1\right]2\pi\bar{\lambda}_{u,t}r_{iza}dr_{iza}\right)}, \quad (36)$$

where the expectation is with respect to r_{iia} and r_{za}. However, r_{iia} follows the distribution of r_{za} as all clusters have similar dimensions. Therefore, we can simplify (36) as

$$M_{I_u}(s) = e^{\left(\sum_{v=1}^\infty \frac{\pi\bar{\lambda}_{u,t}\alpha v}{v!(\alpha v-1)}\left(\frac{-sP_u}{\kappa}\right)^v\left(\frac{d_l^{\alpha v}}{2^{\alpha v-1}(\alpha v+2)}\right)^2\right)}. \quad (37)$$

The expectation and variance of I_u are obtained from the moments of (37) as $\mathbb{E}[I_u] = \frac{\pi\bar{\lambda}_{u,t}\alpha P_u d_l^{2\alpha}}{\kappa(\alpha-1)(2^{\alpha-1}(\alpha+2))^2}$ and $Var[I_u] = \frac{\pi\bar{\lambda}_{u,t}\alpha P_u^2 d_l^{4\alpha}}{\kappa^2(2\alpha-1)(2^{2\alpha}(\alpha+1))^2}$.

2) Voronoi model: We now derive the MGFs of I_p and I_u under the voronoi model for the underlay nodes. Under this model, the distributions of r_{za} and r_{iia} are different. r_{za} has an approximate PDF obtained using similar arguments to r_{jja} which is given by $Ral(\pi\hat{\lambda}_{u,t})$. Now, we can simplify (34) as

$$M_{I_p}(s)=e^{\left(\sum_{v=1}^\infty \frac{\pi\bar{\lambda}_{pt}}{v!}\left(\frac{-sP_pP_{p,u}}{P_{p,p}}\right)^v\left(\frac{\alpha v(\Gamma(\frac{\alpha v}{2}+1))^2}{(\alpha v-1)(\pi\lambda_{p,t})^{\frac{\alpha v}{2}}(\pi\hat{\lambda}_{u,t})^{\frac{\alpha v}{2}}}\right)\right)}, \quad (38)$$

[6]The singularities at $\alpha = 0.5, 1$ are irrelevant as those values do not occur in practical systems.

The mean and variance of I_p are obtained for the voronoi model as $\mathbb{E}[I_p] = \frac{\eta P_pP_{p,u}\alpha(\Gamma(\frac{\alpha}{2}+1))^2}{P_{p,p}(\alpha-1)(\pi\lambda_{p,t})^{\frac{\alpha}{2}-1}(\pi\hat{\lambda}_{u,t})^{\frac{\alpha}{2}}}$ and $Var[I_p] = \frac{2\eta(P_pP_{p,u})^2\alpha(\Gamma(\alpha+1))^2}{P_{p,p}^2(2\alpha-1)(\pi\lambda_{p,t})^{\alpha-1}(\pi\hat{\lambda}_{u,t})^{\alpha}}$.

When deriving $M_{I_u}(s)$, the distribution of r_{iia} is need. However, this follows the same distribution as r_{za} as both involve CU receivers selecting the nearest CU transmitter. Thus, this PDF is given by $Ral(\pi\hat{\lambda}_{u,t})$. With this, we can simplify (36) as

$$M_{I_u}(s) = e^{\left(\sum_{v=1}^\infty \frac{\pi\bar{\lambda}_{u,t}\alpha v}{v!(\alpha v-1)}\left(\frac{-sP_u}{\kappa}\right)^v\left(\frac{\Gamma(\frac{\alpha v}{2}+1)}{(\pi\hat{\lambda}_{u,t})^{\frac{\alpha v}{2}}}\right)^2\right)}. \quad (39)$$

Furthermore, the mean and variance of I_u are obtained as $\mathbb{E}[I_u] = \frac{\theta\alpha P_u(\Gamma(\frac{\alpha}{2}+1))^2}{\kappa(\alpha-1)(\pi\hat{\lambda}_{u,t})^{\alpha-1}}$ and $Var[I_u] = \frac{2\theta\alpha P_u^2(\Gamma(\alpha+1))^2}{\kappa^2(2\alpha-1)(\pi\hat{\lambda}_{u,t})^{2\alpha-1}}$.

Now, in order to evaluate (33), I will be approximated as a gamma distribution using first and second order moment matching [51]. The resulting gamma distribution has shape and scale parameters of $\frac{(\mathbb{E}[I_u]+\mathbb{E}[I_p])^2}{Var[I_u]+Var[I_p]}$ and $\frac{Var[I_u]+Var[I_p]}{\mathbb{E}[I_u]+\mathbb{E}[I_p]}$ respectively. The outage probability of a CU receiver is finally expressed as

$$P_O=1-\frac{1}{\Gamma\left(\frac{(\mathbb{E}[I_u]+\mathbb{E}[I_p])^2}{Var[I_u]+Var[I_p]}\right)}\gamma\left(\frac{(\mathbb{E}[I_u]+\mathbb{E}[I_p])^2}{Var[I_u]+Var[I_p]},\frac{\frac{P_u}{\kappa T}}{\frac{Var[I_u]+Var[I_p]}{\mathbb{E}[I_u]+\mathbb{E}[I_p]}}\right). \quad (40)$$

V. Numerical Results

This section provides numerical outage probability of a CU receiver. We first investigate the single antenna case, followed by the massive MIMO case.

A. Single antenna

For this case, we use the parameters $\lambda_{u,t} = 1\times10^{-5}$, $\lambda_{p,t} = 1\times10^{-5}$, $r = 50$, $R_G = 20$, $P_u = 1\times10^{-8}$, and $\sigma^2 = 0$ [16], [33]. The noise variance is set to zero in order to highlight the effect of interference. We will denote the underlay association scheme where the transmitter selects the closest receiver as Scheme 1, and the receiver selects the closest transmitter as Scheme 2.

Fig. 3 plots the outage probability of a CU receiver with respect to the required SINR threshold. Although the outage probabilities differ significantly for different α when the threshold (T) is low, they converge to 1 as expected when T increases. The outage increase for higher α occurs primarily due to the power control procedures which require an inversion of the path loss. Although the outage of Scheme 2 is higher, the difference is not significant because the main source of interference is the primary network.

The CU receiver outage is plotted vs. the required PU receiver power level P_p in Fig. 4. The plots diverge for lower P_p due to interference from the primary network playing a less dominant role. The outage probabilities drop significantly when the primary and CU receiver densities are increased. For Scheme 1, this is due to the guard region surrounding each PU receiver. For Scheme 2, in addition to this reason, the distance from an interfering CU transmitter to its associated receiver reduces; causing the transmit power to reduce, which in turn reduces interference. Moreover, when the maximum

allowable transmit distance D increases, the outage increases because more associations (requiring higher transmit power) are successful. It is also interesting to note that Scheme 1 shows a worse outage performance compared to Scheme 2 when $D = 200$ and $\lambda_{p,r} = \lambda_{s,r} = 1 \times 10^{-3}$.

We now investigate the performance of the cluster model. Fig. 5 plots the underlay outage with respect to the threshold SINR level. The outage increases significantly when the path loss exponent α increases. Moreover, the rate of outage decrease vs. the threshold is inversely proportional to α. Furthermore, for each value of α, increasing the cluster radius d_l further increases outage. This is due to higher transmit power requirements for CU transmitters. When the threshold increases, the effect of α decreases, and d_l plays a bigger role. For example, above -28 dB, having a cluster radius of 50 and $\alpha = 4$ provides a lower outage than a cluster radius of 500 and $\alpha = 3$.

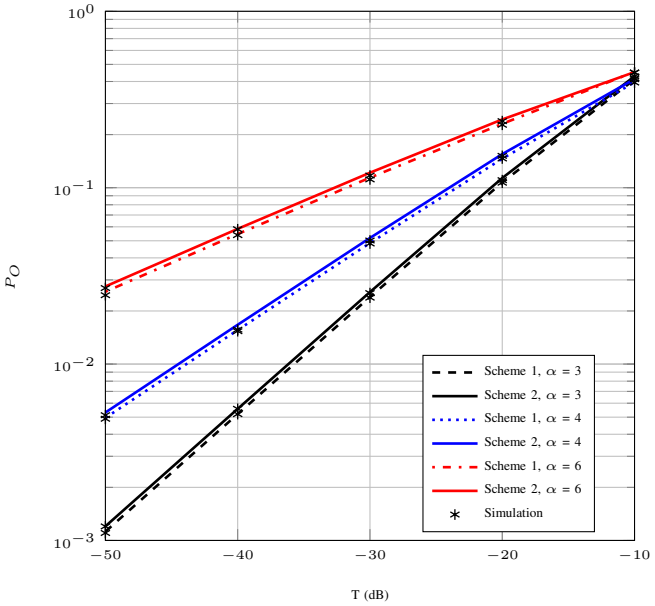

Fig. 3: Outage probability vs. the required SINR threshold T under different path loss exponents α for the two underlay association schemes. $D = 100$, $P_p = 1 \times 10^{-8}$, $\lambda_{p,r} = 1 \times 10^{-4}$, and $\lambda_{s,r} = 1 \times 10^{-4}$.

B. Massive MIMO

This provides numerical results on the outage probability of a CU receiver for different system parameters with massive MIMO base stations. The parameter values are $P_{p,p} = -80$ dBm, $P_{p,u} = -80$ dBm, $P_u = -70$ dBm, $q = 64$, $T = 1$, $R_G = 20$, and $\kappa = 1$ (we have used up towards 500 antennas) unless stated otherwise [11], [33], [54], [55].

We first investigate the cluster model for underlay nodes. As mentioned in Section II, the cluster model is useful for sets of independent pico cells or wireless local area networks underlayed within a cellular network or a terrestrial television network. Fig. 6 plots the variation of the outage probability P_O with respect to the path loss exponent α. As α increases, P_O reduces for all values of P_p and d_l. However, the rate of decline varies slightly with α. Moreover, while having a higher outage probability when other parameter values remain

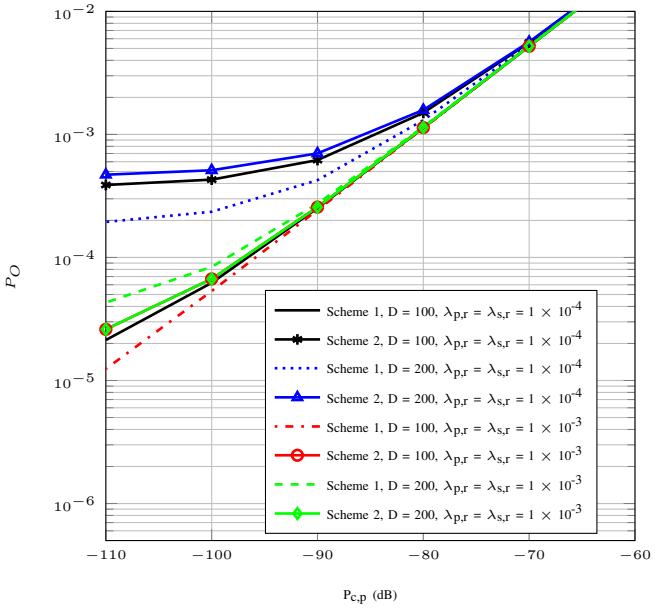

Fig. 4: Outage probability vs. P_p under different $\lambda_{p,r}$, $\lambda_{s,r}$, and D for the two underlay association schemes. $\alpha = 3$, and $T = 0.0001$.

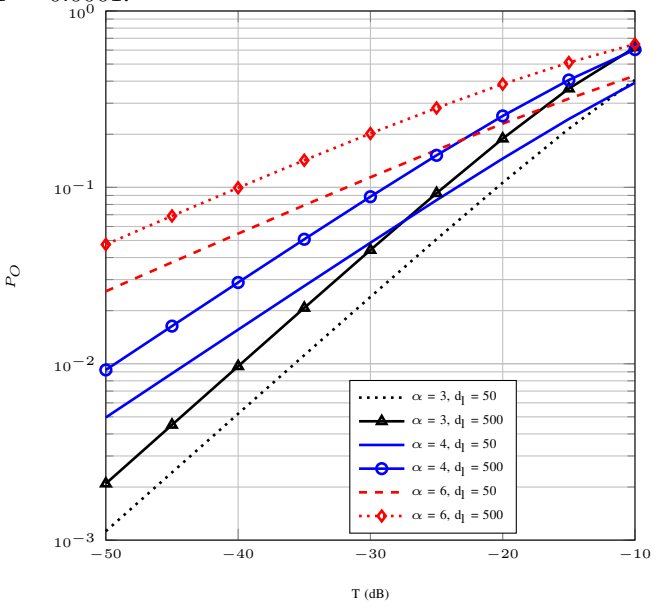

Fig. 5: Outage probability vs. the required SINR threshold T under different path loss exponents α and cluster radii. $P_p = 1 \times 10^{-8}$, $\lambda_{p,r} = 1 \times 10^{-4}$, and $\lambda_{s,r} = 1 \times 10^{-4}$.

the same, a higher d_l also provides a greater outage variation when P_p is varied.

In Fig. 7, the outage probability is plotted with respect to the PU receiver density $\lambda_{p,r}$. The plot shows a complex relationship without a clear trend. However, a higher cluster radius d_l always provides a higher outage. It is interesting to note that at $\lambda_{p,r} \approx -25$ dB, all curves roughly show a similar outage. However, it should be noted that they do not coincide at the same exact value. For very low PU receiver densities, each set of values approach a steady state outage without significant deviation when $\lambda_{p,r}$ changes. However, when $\lambda_{p,r}$ is high, the curves under $\lambda_{p,t} = 10^{-3}$ shows a slight increase before decreasing while all other curves

show a sharp decrease. The total interference is due to the sum of primary and underlay interference. When $\lambda_{p,r}$ is increased, two contradictory effects occur. First, as the area under guard regions increase, there would be less underlay transmitters, and thus less underlay interferers. Second, the proportion of idle primary transmitters with which no receiver is associated with decrease, and thus primary interference is increased. However, for this second effect to be significant, the primary interference should have played a significant role in the first place. Therefore, it is not seen within the curves with $\lambda_{p,t} = 10^{-4}$ for which the underlay interference is the main contributor to the outage. However, when the primary transmitter density is sufficiently high ($\lambda_{p,t} = 10^{-3}$), the primary interference still imparts a considerable impact on the outage, and thus the second effect initially occurs as seen with the increased outage. However, the first effect predominates as $\lambda_{p,r}$ is increased further, and the outage drops.

We now move our attention to the voronoi model for the CU network, which is useful when multiple pico or wireless local area network base stations belonging to the same network cover a particular geographical area. Fig. 8 plots the outage vs. the path loss exponent. While increasing α reduces the outage, the rate of decrease changes with α, and this in turn depends on the specific P_p and P_u values. Furthermore, for high P_u and low P_p values, the outage is significantly lower at low α. Conversely, for low P_u and high P_p, the outage is significantly higher due to the primary interference being comparatively higher with respect to the desired signal power. We can observe that when $P_p = P_u$, the outage does not depend on the actual value of P_p or P_u.

Fig. 9 plots the outage with respect to the CU transmitter density $\lambda_{u,t}$. For all values of $\lambda_{u,r}$, there exists a $\lambda_{u,t}$ value where the outage peaks. Moreover, increasing $\lambda_{p,t}$ pushes the location of the maxima to the right; making it occur at a higher $\lambda_{u,t}$. The reason behind the outage peak is as follows. When the CU transmitter density $\lambda_{u,t}$ increases, the interference increases initially as the number of concurrent transmissions increase, and a rise in the outage occurs. However, when $\lambda_{u,t}$ increases further, the additional CU transmitters will not have an associated receiver. Moreover, an increased $\lambda_{u,t}$ means a lower average cell size, and thus due to the path loss inversion based power control, the transmit power of a CU transmitter reduces. Therefore, even the interference from associated CU transmitters would reduce. The outage peak is significant when $\lambda_{u,r} = 10^{-2}$ while it is insignificant for $\lambda_{u,r} = 10^{-3}$. This is because having a higher $\lambda_{u,r}$ means that the additional CU transmitters would be associated to a receiver, creating interference. Conversely, when $\lambda_{u,r}$ is lower, only a small amount of the additional CU transmitters cause interference. As such, the best way to reduce the outage peak is by having a lower CU receiver density.

We now investigate the effect of the ratio between PU and CU transmitter antennas κ on the outage in Fig. 10. When κ is increased from 1 to 20, the change in outage is not very significant. However, the trends of the change show significant differences with respect to the PU and CU transmitter densities. While showing similar trends, $\lambda_{p,t} = \lambda_{u,t} = 10^{-3}$ has a lower outage than $\lambda_{p,t} = \lambda_{u,t} = 10^{-4}$. Because the PU and CU receiver densities are comparable at 10^{-3}, the additional transmitters do not get associated with a receiver. Furthermore, the shrinking of cell size causes the transmit power to drop, reducing interference.

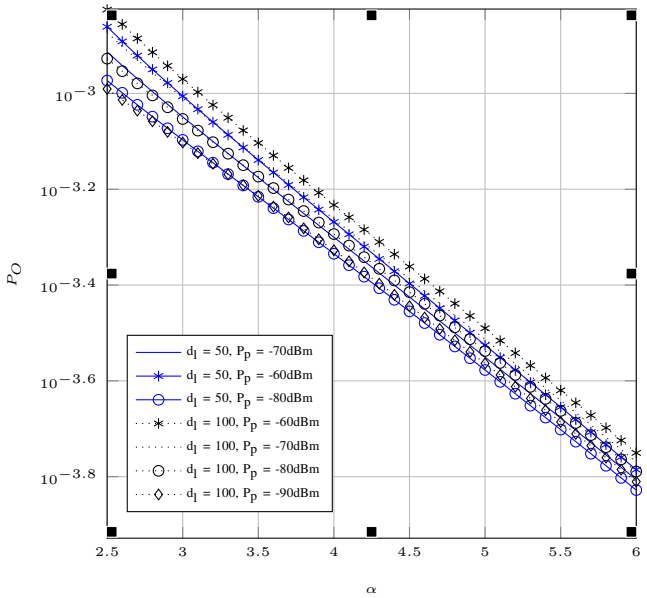

Fig. 6: Outage probability vs. the path loss exponent (α) for different values of d_l and P_p for the cluster model. $\lambda_{p,t} = 10^{-4}$, $\lambda_{u,t} = 10^{-4}$, $\lambda_{p,r} = 10^{-2}$, $\lambda_{u,r} = 10^{-2}$.

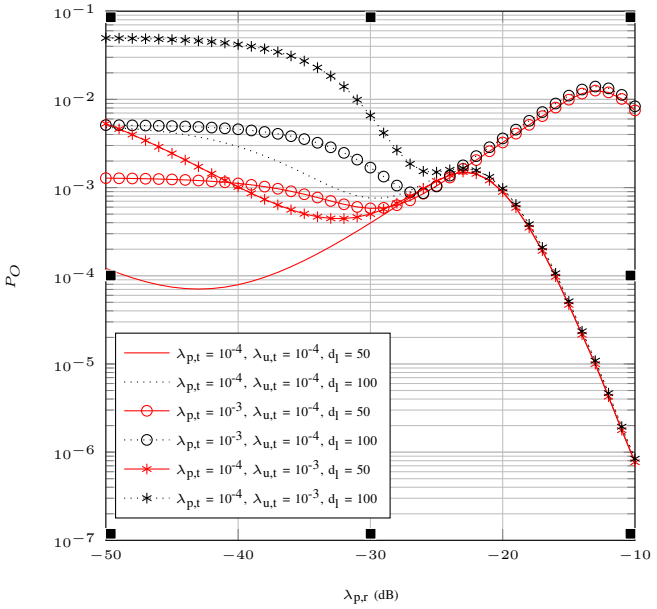

Fig. 7: Outage probability vs. the PU receiver density ($\lambda_{p,r}$) under different values of $\lambda_{p,t}$, $\lambda_{u,t}$, and d_l for the cluster model. $\alpha = 3$, $P_p = -70$ dBm, and $\lambda_{u,r} = 10^{-2}$.

VI. Conclusion

This paper analyzed the aggregate interference on a CU receiver from primary and other underlay base stations when the interfering base stations are single antenna type or massive MIMO. We considered a path loss inversion based power

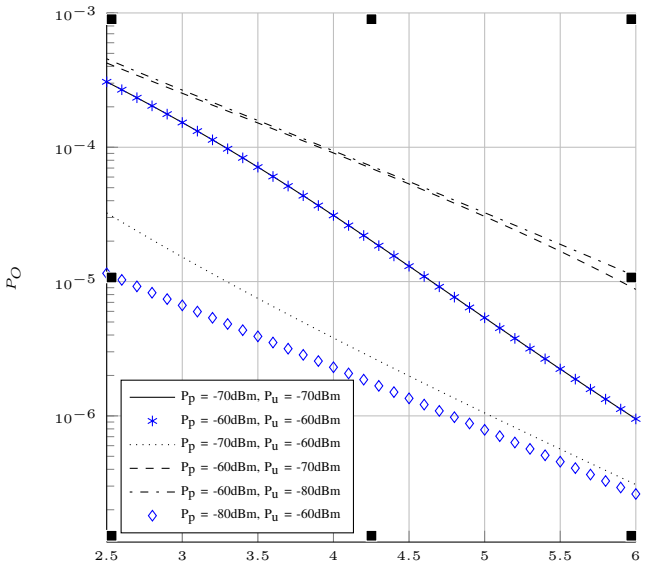

Fig. 8: Outage probability vs. the path loss exponent (α) for different values of P_u and P_p for the voronoi model. $\lambda_{p,t} = 10^{-4}$, $\lambda_{u,t} = 10^{-4}$, $\lambda_{p,r} = 10^{-3}$, and $\lambda_{u,r} = 10^{-2}$.

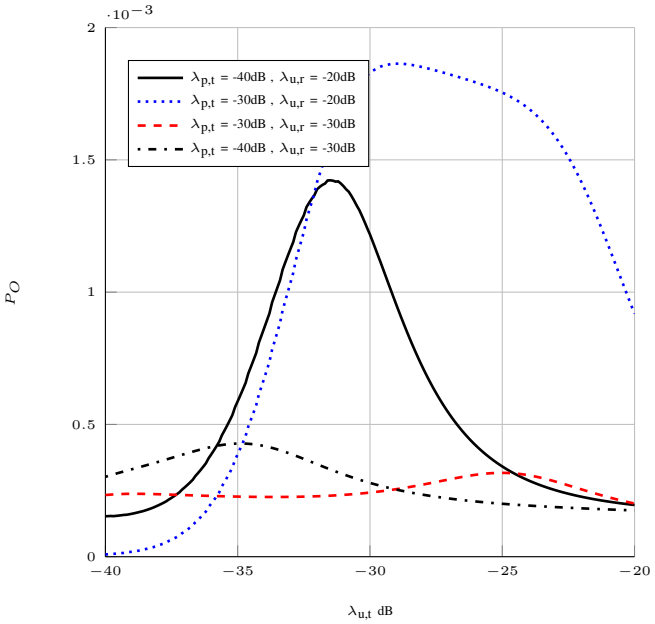

Fig. 9: Outage probability vs. the CU transmitter density ($\lambda_{u,t}$) under different values of $\lambda_{p,t}$ and $\lambda_{u,r}$ for the voronoi model. $\alpha = 3$, $P_p = -70$ dBm, and $\lambda_{p,r} = 10^{-3}$.

control scheme for transmitting the pilot signals as well as the primary and underlay data signals. The PU transmitters and receivers were modeled as homogeneous PPPs in $\mathbb{R}^2$ while the underlay network was modeled in two ways: 1) as a Matern cluster process with the cluster centres representing base stations, and 2) as homogeneous PPPs in $\mathbb{R}^2$. All processes were assumed to be stationary. Moreover, two underlay association schemes were analyzed and exclusion regions around the PU receivers were considered.

The MGF of the aggregate interference on a CU receiver and its outage probability were derived for both single antenna scenarios and massive MIMO scenarios under pilot contamination. For the single antenna case, the interference from the primary system was shown to be independent of the node densities. Furthermore, when the required power threshold for the PU receiver (P_p) is comparative with the required underlay threshold (P_u), interference from the primary system dominates, and the path loss exponent greatly affects the outage. However, when $P_p < P_u$, the outage is significantly affected by the receiver densities and the maximum allowable underlay transmit distance. Moreover, increasing the cluster radius significantly increases the outage. For the massive MIMO case, it was observed that while an increased path loss exponent reduced the outage, the rate of decrease varied with threshold power levels and system parameters. Furthermore, transmitter densities of both networks significantly affected the outage characteristics, and a specific CU transmitter density maximizes the outage probability. Furthermore, when the thresholds P_p and P_u are equal, the outage does not depend on the exact value of either.

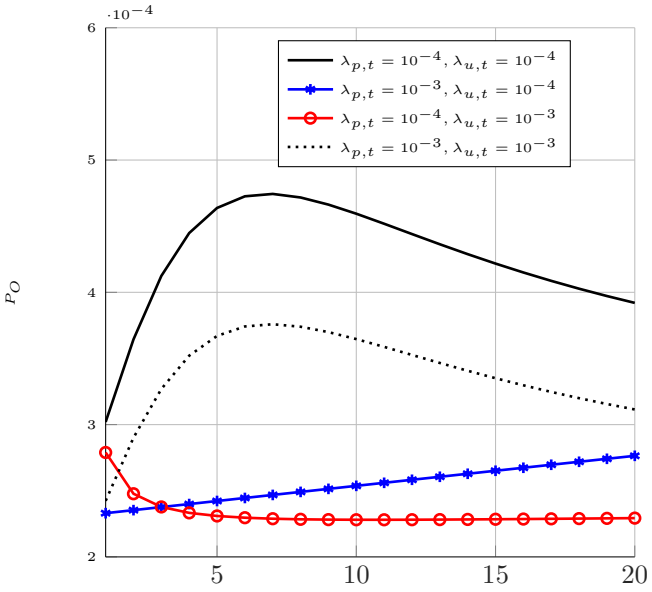

Fig. 10: Outage probability vs. the ratio between PU and CU transmitter antennas (κ) under different values of $\lambda_{p,t}$ and $\lambda_{u,t}$ for the voronoi model. $\alpha = 3$, $P_p = -70$ dBm, $\lambda_{p,r} = 10^{-3}$, and $\lambda_{u,r} = 10^{-3}$.

APPENDIX
PROOF OF $f_{r_{p,tx}}(x)$

The 1-D intensity of PU receivers with respect to a PU transmitter ($\tilde{\lambda}_{p,r}$) is $\tilde{\lambda}_{p,r} = 2\pi\lambda_{p,r}r, 0 < r < \infty$. Let ν be the probability that any PU receiver has the PU transmitter concerned as the closest PU transmitter. We assume ν is independent for each PU receiver. Using the Coloring Theorem [46], we can perform independent thinning on the process of PU receivers to obtain the intensity of the process of PU receivers which have the given PU transmitter as the closest ($\bar{\lambda}$). $\bar{\lambda}$ is given by $\bar{\lambda} = \nu\tilde{\lambda}$. To find ν, we need to use the void probability for PPPs. In other words, there should be 0 PU transmitters within an annular area of radius r. The probability of having n nodes within a given area A is [56] $P(n) = \frac{(\lambda_{p,t}A)^n}{n!}e^{-\lambda_{p,t}A}$. Therefore, ν is obtained as $\nu =$

$e^{-\pi\lambda_{p,t}r^2}$, and $\bar{\lambda}$ is derived as $\bar{\lambda} = 2\pi\lambda_{p,r}r_{p,tx}e^{-\pi\lambda_{p,t}r_{p,tx}^2}$, where $r_{p,tx}$ was substituted for r. The CDF of $r_{p,tx}$ is given by

$$F_{r_{p,tx}}(x) = \frac{\int_{r_{p,tx}=0}^{x} \bar{\lambda} dr}{\int_{r_{p,tx}=0}^{\infty} \bar{\lambda} dr} = 1 - e^{-\pi\lambda_{p,t}x^2}. \quad (41)$$

Differentiating (41) gives the PDF.

REFERENCES

[1] S. Kusaladharma and C. Tellambura, "Massive MIMO based underlay networks with power control," in *Proc. IEEE ICC*, May 2016, pp. 1–6.

[2] S. Kusaladharma, P. Herath, and C. Tellambura, "Secondary user interference characterization for underlay networks," in *Proc. IEEE VTC*, Sept 2015, pp. 1–5.

[3] S. Srinivasa and S. Jafar, "Cognitive radios for dynamic spectrum access - the throughput potential of cognitive radio: A theoretical perspective," *IEEE Commun. Mag.*, vol. 45, no. 5, pp. 73–79, May 2007.

[4] C.-X. Wang, F. Haider, X. Gao, X.-H. You, Y. Yang, D. Yuan, H. Aggoune, H. Haas, S. Fletcher, and E. Hepsaydir, "Cellular architecture and key technologies for 5g wireless communication networks," *IEEE Commun. Magazine*, vol. 52, no. 2, pp. 122–130, February 2014.

[5] A. Gupta and R. Jha, "A survey of 5g network: Architecture and emerging technologies," *IEEE Access*, vol. 3, pp. 1206–1232, 2015.

[6] X. Hong, J. Wang, C.-X. Wang, and J. Shi, "Cognitive radio in 5G: a perspective on energy-spectral efficiency trade-off," *IEEE Commun. Magazine*, vol. 52, no. 7, pp. 46–53, July 2014.

[7] S. Atapattu, C. Tellambura, and H. Jiang, *Energy Detection for Spectrum Sensing in Cognitive Radio*. Springer, 2014.

[8] S. Kusaladharma and C. Tellambura, "On approximating the cognitive radio aggregate interference," *IEEE Wireless Commun. Lett.*, vol. 2, no. 1, pp. 58–61, 2013.

[9] V. Jungnickel, K. Manolakis, W. Zirwas, B. Panzner, V. Braun, M. Lossow, M. Sternad, R. Apelfro, and T. Svensson, "The role of small cells, coordinated multipoint, and massive MIMO in 5G," *Communications Magazine, IEEE*, vol. 52, no. 5, pp. 44–51, May 2014.

[10] S. Schwarz, M. Wrulich, and M. Rupp, "Mutual information based calculation of the precoding matrix indicator for 3gpp umts/lte," in *Proc. IEEE WSA*, Feb 2010, pp. 52–58.

[11] P. Madhusudhanan, X. Li, Y. Liu, and T. Brown, "Stochastic geometric modeling and interference analysis for massive MIMO systems," in *Proc. IEEE WiOpt*, May 2013, pp. 15–22.

[12] Q. Ye, O. Y. Bursalioglu, H. C. Papadopoulos, C. Caramanis, and J. G. Andrews, "User association and interference management in massive MIMO hetnets," *IEEE Trans. Commun.*, vol. 64, no. 5, pp. 2049–2065, May 2016.

[13] C. Feng, Y. Jing, and S. Jin, "Interference and outage probability analysis for massive MIMO downlink with MF precoding," *IEEE Signal Process. Lett.*, vol. 23, no. 3, pp. 366–370, March 2016.

[14] A. Adhikary, H. S. Dhillon, and G. Caire, "Massive-MIMO meets hetnet: Interference coordination through spatial blanking," *IEEE J. Sel. Areas Commun.*, vol. 33, no. 6, pp. 1171–1186, June 2015.

[15] C.-H. Lee and M. Haenggi, "Interference and outage in poisson cognitive networks," *IEEE Trans. Wireless Commun.*, vol. 11, no. 4, pp. 1392–1401, Apr. 2012.

[16] S. Kusaladharma, P. Herath, and C. Tellambura, "Underlay interference analysis of power control and receiver association schemes," *IEEE Trans. Veh. Technol.*, vol. 65, no. 11, pp. 8978–8991, 2016.

[17] Z. Chen, C.-X. Wang, X. Hong, J. Thompson, S. Vorobyov, X. Ge, H. Xiao, and F. Zhao, "Aggregate interference modeling in cognitive radio networks with power and contention control," *IEEE Trans. Commun.*, vol. 60, no. 2, pp. 456–468, Feb. 2012.

[18] M. Peng, Y. Li, T. Quek, and C. Wang, "Device-to-device underlaid cellular networks under Rician fading channels," *IEEE Trans. Wireless Commun.*, vol. 13, no. 8, pp. 4247–4259, Aug 2014.

[19] S. Zaidi, D. McLernon, and M. Ghogho, "Breaking the area spectral efficiency wall in cognitive underlay networks," *IEEE J. Sel. Areas Commun.*, vol. PP, no. 99, pp. 1–17, 2014.

[20] C. Sun, Y. Alemseged, H.-N. Tran, and H. Harada, "Transmit power control for cognitive radio over a Rayleigh fading channel," *IEEE Trans. Veh. Technol.*, vol. 59, no. 4, pp. 1847–1857, 2010.

[21] Z. Wang and W. Zhang, "Spectrum sharing with limited feedback in poisson cognitive network," in *Proc. IEEE ICC*, June 2014, pp. 1441–1446.

[22] M. J. Rahman and X. Wang, "Probabilistic analysis of mutual interference in cognitive radio communications," in *Proc. IEEE GLOBECOM*, Dec. 2011, pp. 1–5.

[23] S. Govindasamy, "Uplink performance of large optimum-combining antenna arrays in poisson-cell networks," in *Proc. IEEE ICC*, June 2014, pp. 2158–2164.

[24] M. Kountouris and N. Pappas, "Hetnets and massive MIMO: Modeling, potential gains, and performance analysis," in *Proc. IEEE APWC*, Sept 2013, pp. 1319–1322.

[25] X. Zou, G. Cui, M. Tang, and W. Wang, "Base station density bounded by maximum outage probability in massive MIMO system," in *Proc. IEEE VTC*, May 2015, pp. 1–5.

[26] X. Lin, R. W. Heath, and J. G. Andrews, "The interplay between massive MIMO and underlaid D2D networking," *IEEE Trans. Wireless Commun.*, vol. 14, no. 6, pp. 3337–3351, June 2015.

[27] S. Shalmashi, E. Bjornson, M. Kountouris, K. W. Sung, and M. Debbah, "Energy efficiency and sum rate when massive MIMO meets device-to-device communication," in *Proc. IEEE ICCW*, June 2015, pp. 627–632.

[28] I. Gradshteyn and I. Ryzhik, *Table of integrals, Series, and Products*, 7th ed. Academic Press, 2007.

[29] H. Dhillon, R. Ganti, F. Baccelli, and J. Andrews, "Modeling and analysis of k-tier downlink heterogeneous cellular networks," *IEEE J. Sel. Areas Commun.*, vol. 30, no. 3, pp. 550–560, April 2012.

[30] E. Salbaroli and A. Zanella, "Interference analysis in a Poisson field of nodes of finite area," *IEEE Trans. Veh. Technol.*, vol. 58, no. 4, pp. 1776–1783, May 2009.

[31] A. Rabbachin, T. Q. S. Quek, H. Shin, and M. Z. Win, "Cognitive network interference," *IEEE J. Sel. Areas Commun.*, vol. 29, no. 2, pp. 480–493, Feb. 2011.

[32] S.-R. Cho and W. Choi, "Coverage and load balancing in heterogeneous cellular networks with minimum cell separation," *IEEE Trans. Mobile Computing*, vol. 13, no. 9, pp. 1955–1966, Sept 2014.

[33] L. Vijayandran, P. Dharmawansa, T. Ekman, and C. Tellambura, "Analysis of aggregate interference and primary system performance in finite area cognitive radio networks," *IEEE Trans. Commun.*, vol. PP, no. 99, pp. 1–12, 2012.

[34] A. Baddeley, I. Barany, R. Schneider, and W. Weil, *Spatial Point Processes and their Applications*. Springer, 2007.

[35] N. Deng, W. Zhou, and M. Haenggi, "Heterogeneous cellular network models with dependence," *IEEE J. Sel. Areas Commun.*, vol. 33, no. 10, pp. 2167–2181, Oct 2015.

[36] Y. Liu, C. Yin, J. Gao, and X. Sun, "Transmission capacity for overlaid wireless networks: A homogeneous primary network versus an inhomogeneous secondary network," in *Proc. IEEE ICCCAS*, vol. 1, Nov 2013, pp. 154–158.

[37] Y. Zhou, Z. Zhao, Q. Ying, R. Li, X. Zhou, and H. Zhang, "Two-tier spatial modeling of base stations in cellular networks," in *Proc. IEEE PIMRC*, Sept 2014, pp. 1570–1574.

[38] A. Goldsmith, *Wireless Communications*. Cambridge University Press, 2005.

[39] A. Molisch, *Wireless Communications*. Wiley-IEEE Press, 2011.

[40] M. Haenggi, *Stochastic Geometry for Wireless Networks*. Cambridge University Press, 2013.

[41] Y. G. Lim, C. B. Chae, and G. Caire, "Performance analysis of massive MIMO for cell-boundary users," *IEEE Trans. on Wireless Commun.*, vol. 14, no. 12, pp. 6827–6842, Dec 2015.

[42] J. Jose, A. Ashikhmin, T. L. Marzetta, and S. Vishwanath, "Pilot contamination and precoding in multi-cell TDD systems," *IEEE Trans. on Wireless Commun.*, vol. 10, no. 8, pp. 2640–2651, August 2011.

[43] C. Tellambura, A. J. Mueller, and V. K. Bhargawa, "Analysis of M-ary phase-shift keying with diversity reception for land-mobile satellite channels," *IEEE Transactions on Vehicular Technology*, vol. 46, no. 4, pp. 910–922, Nov 1997.

[44] C. Tellambura, A. Annamalai, and V. K. Bhargava, "Closed form and infinite series solutions for the MGF of a dual-diversity selection combiner output in bivariate Nakagami fading," *IEEE Transactions on Communications*, vol. 51, no. 4, pp. 539–542, April 2003.

[45] C. Tellambura, "Evaluation of the exact union bound for trellis-coded modulations over fading channels," *IEEE Transactions on Communications*, vol. 44, no. 12, pp. 1693–1699, Dec 1996.

[46] J. F. Kingman, *Poisson Processes*. Oxford University Press, 1993.

[47] B. Yu, L. Yang, H. Ishii, and S. Mukherjee, "Dynamic TDD support in macrocell-assisted small cell architecture," *IEEE J. Sel. Areas Commun.*, vol. 33, no. 6, pp. 1201–1213, June 2015.

[48] D. Moltchanov, "Distance distributions in random networks," *Ad Hoc Networks*, vol. 10, no. 6, pp. 1146–1166, 2012. [Online]. Available: http://www.sciencedirect.com/science/article/pii/S1570870512000224

[49] B. Yu, S. Mukherjee, H. Ishii, and L. Yang, "Dynamic TDD support in the LTE-B enhanced local area architecture," in *Proc. IEEE GLOBECOM*, Dec 2012, pp. 585–591.

[50] Z. Yazdanshenasan, H. S. Dhillon, M. Afshang, and P. H. J. Chong, "Poisson hole process: Theory and applications to wireless networks," *IEEE Trans. Wireless Commun.*, vol. 15, no. 11, pp. 7531–7546, Nov 2016.

[51] S. Kusaladharma and C. Tellambura, "Aggregate interference analysis for underlay cognitive radio networks," *IEEE Wireless Commun. Lett.*, vol. 1, no. 6, pp. 641–644, 2012.

[52] J. Ferenc and Z. Neda, "On the size distribution of poisson voronoi cells," *Phisica A: Statistical Mechanics and its Applications*, vol. 385, no. 2, pp. 518–526, Nov 2007.

[53] T. Novlan, H. Dhillon, and J. Andrews, "Analytical modeling of uplink cellular networks," *IEEE Trans. Wireless Commun.*, vol. 12, no. 6, pp. 2669–2679, June 2013.

[54] Z. Chen, L. Qiu, and X. Liang, "Area spectral efficiency analysis and energy consumption minimization in multiantenna poisson distributed networks," *IEEE Trans. Wireless Commun.*, vol. 15, no. 7, pp. 4862–4874, July 2016.

[55] M. Xie, X. Jia, M. Zhou, and L. Yang, "Study on energy efficiency of D2D underlay massive MIMO networks with power beacons," in *Proc. IEEE WCSP*, Oct 2016, pp. 1–5.

[56] D. Stoyan, W. S. Kendall, and J. Mecke, *Stochastic Geometry and Its Applications*. Wiley, 1996.